

NBER WORKING PAPER SERIES

THE UNSEEN COSTS OF BLUE SKIES:
POLLUTANT SUBSTITUTION AND BIODIVERSITY LOSS

Joshua S. Graff Zivin
Siyuan Li
Huanhuan Wang
Zhiqiang Zhang

Working Paper 35087
<http://www.nber.org/papers/w35087>

NATIONAL BUREAU OF ECONOMIC RESEARCH
1050 Massachusetts Avenue
Cambridge, MA 02138
April 2026

We acknowledge financial support from the Key Research Program of National Social Science Fund (No. 25AJL019) and the National Natural Science Foundation of China (72433002, 7250030619 and 72503049). The views expressed herein are those of the authors and do not necessarily reflect the views of the National Bureau of Economic Research.

NBER working papers are circulated for discussion and comment purposes. They have not been peer-reviewed or been subject to the review by the NBER Board of Directors that accompanies official NBER publications.

© 2026 by Joshua S. Graff Zivin, Siyuan Li, Huanhuan Wang, and Zhiqiang Zhang. All rights reserved. Short sections of text, not to exceed two paragraphs, may be quoted without explicit permission provided that full credit, including © notice, is given to the source.

The Unseen Costs of Blue Skies: Pollutant Substitution and Biodiversity Loss
Joshua S. Graff Zivin, Siyuan Li, Huanhuan Wang, and Zhiqiang Zhang
NBER Working Paper No. 35087
April 2026
JEL No. D73, H77, Q53, Q57, Q58

ABSTRACT

Incomplete performance metrics distort incentives. Exploiting the staggered roll-out of China's national air monitoring network, we document a pollutant substitution effect: PM_{2.5} fell significantly, yet O₃ surged. We trace this to strategic behavior: facing binding PM_{2.5} targets, local governments prioritized abatement of particulate precursors while neglecting ozone precursors. Critically, this was not a benign trade-off. Although the policy reduced PM_{2.5}-attributed deaths, the policy-induced O₃ surge increased O₃-attributed mortality and reduced biodiversity (measured by bird abundance). Conservative estimates suggest these costs reduced the policy's net benefits by approximately 23.8%. Our findings highlight the hidden social costs of narrow performance targeting.

Joshua S. Graff Zivin
University of California, San Diego
and NBER
jgraffzivin@ucsd.edu

Siyuan Li
Fudan University
School of Economics
23110680011@m.fudan.edu.cn

Huanhuan Wang
East China Normal University
School of Economics and Management,
and School of Law
hhwang@law.ecnu.edu.cn

Zhiqiang Zhang
Shanghai International Studies University
School of Economics and Finance
2025001@shisu.edu.cn

1 Introduction

Air pollution control is typically organized as a delegated responsibility: central governments set environmental targets, then subnational governments implement policies to achieve them. This delegation naturally creates a principal–agent relationship, especially when local pollution abatement efforts are difficult to observe or outcomes are imperfectly monitored. A large literature documents that local officials often respond strategically under such incentive schemes—for example, by misreporting data or shifting pollution-generating activities away from monitors (Ghanem and Zhang, 2014; Chen et al., 2018; He et al., 2020; Zou, 2021; Yang et al., 2024). Beyond these classic hidden-action responses, a growing body of evidence shows that narrow, pollutant-specific regulations can induce substitution across environmental dimensions. For instance, Gibson (2019) found that stricter air regulations in the United States led firms to increase water pollution and to shift emissions across locations. But the core governance challenge we highlight extends beyond hidden action on a single pollutant. Ambient air quality is determined by multiple pollutants, whose sources and abatement strategies only partially overlap. When policy attention centers on one pollutant, local officials can improve that metric by shifting emissions or abatement efforts across pollutants, producing the kind of leakage or substitution that yields measured gains on the targeted pollutant even as overall environmental quality may worsen. This is a classic multi-task principal–agent distortion (Holmström and Milgrom, 1991), in which incentivizing one task encourages agents to neglect (or even opportunistically relax) other tasks.¹

China’s recent War on Pollution provides a stark real-world setting in which to examine this multitask governance problem. Beginning in 2013, the central government launched an ambitious campaign centered on binding particulate-matter reduction targets and a nationwide monitoring network to track compliance. Each province and city received specific PM_{2.5} or PM₁₀ mandates, such as the 25 percent PM_{2.5} reduction requirement for Beijing–Tianjin–Hebei, embedded in responsibility contracts that shaped cadre evaluations.²

¹Most of the literature in the field of environmental governance focuses on pollution leakage, which typically refers to the movement of pollutant emissions across different jurisdictions. While the pollutant substitution we document in this paper receives relatively less attention, we conceptualize it as a type of leakage across pollutants within the same jurisdiction. That is why we regard it as a principal-agent problem and not merely a matter of jurisdictional authority.

²The targets are determined based on population density and the historical levels of pollution. For instance,

The accountability system, however, focused almost entirely on particulates: other pollutants, including ozone (O_3), were not subject to formal targets.

At the same time, China rolled out a large monitoring network, installed in stages between 2013 and 2015, that eventually covered 338 cities with more than 1,400 stations. More than 94 percent of these monitors were placed in built-up urban areas, leaving rural and peri-urban regions largely unmonitored. This combination of one-pollutant targets and spatially concentrated monitoring created strong incentives for local governments to focus their abatement efforts on monitored pollutants and monitored locations.

This paper provides the first comprehensive causal assessment of how this accountability system reshaped China's pollution portfolio. We show that the War on Pollution successfully reduced particulates where monitors were present, but these gains were accompanied by systematic cross-pollutant substitution and spatial displacement—precisely the distortions predicted by the multitask principal-agent framework. Using high-resolution satellite data for $PM_{2.5}$ and O_3 , we document substantial divergence in pollution trends across pollutants and across monitored versus unmonitored areas, and we trace the consequences of these distortions for atmospheric chemistry, ecological outcomes, and social welfare.

Our empirical analysis relies on a unified dataset that combines satellite-derived $PM_{2.5}$ and O_3 concentrations from 2010–2019 with detailed information on the timing and geography of China's monitoring rollout. These satellite data provide consistent coverage across both city centers and rural areas, allowing us to observe pollution even outside the ground monitors' coverage areas. We exploit this dataset in a difference-in-differences framework that leverages two sources of variation. First, we use the staggered installation of national air-quality monitors, which brought some cities under binding particulate-matter targets earlier than others, creating quasi-experimental variation in treatment timing. Second, we compare pollution trends in treated areas—urban locales with monitors and binding PM targets—to those in nearby rural areas that remained unmonitored throughout the rollout. This design allows us to recover the causal impact of the War on Pollution on both targeted and untargeted pollutants, and to detect strategic spatial and cross-pollutant shifts in envi-

the Beijing–Tianjin–Hebei region features one of the densest populations, the most prosperous economy, and the most severe air pollution in China, and thus it has the highest emission reduction target. We will provide more detailed information in Section 2.

ronmental performance.

We find stark evidence of multitask distortions in pollution control. In the years following the policy, particulate concentrations fell sharply in monitored urban areas relative to rural controls, but ozone levels rose almost commensurately. Our estimates indicate that monitor installation and PM target enforcement reduced annual average PM_{2.5} by roughly 0.6 $\mu\text{g m}^{-3}$ while increasing O₃ by a similar magnitude in the same locations. These trade-offs are not attributable to pre-existing trends: the divergences appear only after 2013, coincide with monitor activation, and do not arise in placebo periods. The results are likewise robust to including baseline city characteristics, redefining treatment boundaries, and applying recent estimators for staggered adoption (Goodman-Bacon, 2021; Borusyak et al., 2024).

Why did this happen? We build a simple model to argue that the political economy of incentives in China’s environmental governance drove local officials to strategically reallocate effort across pollutants, consistent with a multitask principal–agent framework.³ Facing intense pressure to meet centrally mandated PM_{2.5} targets, local governments prioritized abatement of the most salient and easily controlled sources of particulate pollution—even if doing so meant neglecting other pollutants. Two patterns support this interpretation. First, areas under greater pre-existing accountability pressure achieved disproportionately larger PM_{2.5} reductions and disproportionately larger O₃ increases. Second, emissions data reveal a sharp decline in SO₂ (a key PM precursor), no meaningful change in NO_x, and appreciable increases in VOCs, a shift that pushed local atmospheric chemistry toward ozone formation (Li et al., 2021). Together, these behavioral and chemical patterns point to the same conclusion: in response to one-dimensional incentives, local officials selected abatement strategies that reduced targeted particulates while enabling conditions that promoted ozone formation.

From a societal perspective, the resulting increases in ozone are a serious concern. O₃ is a harmful pollutant with well-documented effects on human health and natural ecosystems (Hillstrom and Lindroth, 2008; Agathokleous et al., 2020; Wang et al., 2025). To quantify these broader consequences, we examine impacts on bird diversity — a modern-day version of the “canary in the coalmine” that reflects broader ecological health. We use bird

³Appendix H presents the details of the model.

diversity as a proxy for ecological health because birds are widely recognized as valuable indicator species (Liang et al., 2020). Moreover, bird observation data offer three critical advantages for our quantitative analysis: high temporal resolution, extensive spatial coverage, and broad taxonomic representation—features that collectively bolster the robustness and validity of our findings. Using detailed survey data, we find that treated areas experienced significant declines in bird abundance and bird species richness relative to control areas, driven primarily by small-bodied species more vulnerable to ozone exposure. Further analysis confirms that policy-induced O₃ increases are the primary driver of these losses, highlighting ecological losses that remain invisible when policy performance is judged solely by improvements in particulate matter.

To place these effects in a broader welfare context, we perform a back-of-the-envelope calculation that quantifies the health gains from PM_{2.5} reductions and the costs associated with higher ozone levels. Our estimates imply that O₃-related damages offset roughly 23–24 percent of the health benefits from particulate-matter improvements. Although we only capture a subset of ozone’s ecological and health impacts, our findings illustrate how these unintended consequences can alter the social returns from regulation as a result of pollutant substitution. Taken together, these findings show how a narrowly targeted accountability system can generate real improvements in the regulated pollutant while simultaneously inducing distortions that reduce the policy’s net social benefits. A more comprehensive monitoring and incentive system—one that encompasses multiple pollutants and incorporates ecological indicators—would better align local actions with society’s broader environmental objectives and mitigate classic multitask principal–agent failures in pollution governance.

This study makes substantive contributions to three distinct categories of scholarly literature. First, we advance understanding of the political economy of regulation by showing how narrow performance metrics can reshape both how agents pursue a task and which outputs they produce. Across many regulatory domains, one-dimensional accountability systems have been shown to generate strategic responses: schools faced with high-stakes testing reallocate instructional time or focus narrowly on students near proficiency thresholds (Jacob and Levitt, 2003; Figlio and Winicki, 2005; Neal and Whitmore Schanzenbach, 2010), hospitals and insurers adjust behavior in response to public report cards or risk-

adjusted payments by avoiding high-risk patients or upcoding diagnoses (Dranove et al., 2003; Geruso and Layton, 2020), banks restructure balance sheets to meet regulatory ratios without reducing underlying risk (Acharya et al., 2013), and job-training agencies cream-skim easier clients to satisfy placement targets (Heckman et al., 2002). These studies document how performance metrics can distort the measured task. Our paper shows that such metrics can also distort the mix of outputs agents choose to produce. In the context of environmental governance, particulate-matter targets induced officials to reoptimize policies and practices across pollutants, improving the regulated outcome while allowing unregulated pollutants to rise. By demonstrating empirically how incentive design can shift effort across tasks in a multi-output setting—not merely within a single task—we extend the principal–agent literature to a broader class of regulatory distortions.

Second, we extend research on environmental regulation and policy evaluation by identifying pollutant substitution as a previously underappreciated mechanism of implementation failure. Existing work has shown that well-designed regulations can reduce pollution and bring co-benefits, while weak monitoring or misaligned incentives can limit their effectiveness (Shimshack, 2014; Duflo et al., 2018; Qian et al., 2021; Barwick et al., 2024). A related line of work demonstrated that targeted environmental rules can induce firms or individuals to shift emissions to unregulated media or locations (Bi, 2017; Gibson, 2019; Balboni and Shapiro, 2025; Feng et al., 2025; Hong and Chen, 2026), while similar studies discussed optimal abatement policy design after considering the interrelationships among pollutants (Ambec and Coria, 2013; Fullerton and Karney, 2018). While a vast literature focuses on pollution leakage, which typically refers to the movement of pollutant emissions between regulated and unregulated regions, the phenomenon we examine receives less attention. We conceptualize the pollutant substitution as a type of leakage across pollutants within the same jurisdiction, a distortion driven by the multitask principal–agent incentives rather than by limits on jurisdictional authority. Our findings build on the typical insight of pollutant leakage research by showing that similar substitutions can arise within government itself: policy success on a targeted pollutant can mask offsetting increases in untargeted pollutants, yielding an overly optimistic view of regulatory effectiveness when evaluation focuses on a single metric. By quantifying these cross-pollutant effects and incorporating

ecological outcomes into the welfare calculus, we demonstrate the importance of evaluating environmental policies using a broad set of environmental indicators rather than a single pollutant.

Finally, we contribute to the literature on the economics of biodiversity and ecosystem services. While ecological research has long documented biodiversity loss and its drivers (Purvis and Hector, 2000; Richard et al., 2021; Uchida et al., 2025; Marder et al., 2025), the economic literature has only recently begun to systematically study biodiversity outcomes, often hampered by data and identification challenges. Recent economic studies have begun to link human activities to wildlife biodiversity—for example, ozone’s effects on birds (Liang et al., 2020), light pollution’s disruption of sea turtle navigation (Brei et al., 2016), infrastructure-related impacts on bird and marine populations (Meng et al., 2025; Taylor and Mayer, 2023), and the social costs of deteriorating biodiversity (Frank, 2024; Frank and Sudarshan, 2024). We add to this knowledge by integrating high-resolution ecological data into a quasi-experimental economic framework. To our knowledge, this is one of the first studies to trace a causal chain from a large-scale environmental policy, through changes in pollutant concentrations and atmospheric chemistry, to measured biodiversity outcomes. In doing so, we show that policies not explicitly aimed at wildlife can nonetheless have quantifiable biodiversity consequences.

The remainder of the paper is organized as follows. Section 2 provides background on China’s War on Pollution and develops a conceptual framework for multitask incentive problems in this context. Section 3 outlines our data sources and empirical strategy. Section 4 presents the main results on pollutant substitution and explores the mechanisms behind it. Section 5 examines the ecological consequences for biodiversity. Section 6 provides a back-of-the-envelope calculation of the net benefits associated with changes in PM_{2.5} and ozone pollution induced by the policy. Section 7 concludes with policy implications and directions for future research.

2 Institutional Background and Hypotheses

2.1 The “War on Pollution” and Its Target-Based Framework

Amid rapid urbanization and industrialization, China has faced a severe air pollution crisis. A vast body of research identifies fine particulate matter as a primary public health threat, with long-term exposure significantly increasing the risk of respiratory, cardiovascular, and neurological diseases (Southerland et al., 2022), as well as reducing life expectancy (Cohen et al., 2017; Ebenstein et al., 2017). In response to this urgent public health crisis and strong public demand for clean air, the Chinese government declared a “War on Pollution” beginning in 2013, elevating environmental protection to an unprecedented strategic priority through a series of significant institutional reforms. The core of these reforms was to rapidly reduce particulate matter concentrations in densely populated areas by strengthening performance accountability and information disclosure.

This governance framework, built upon a series of key measures, exhibits two features that are crucial for our study:

A Singular Focus on Particulate Matter. In response to society’s concern over smog, the primary focus of the 2013 “Air Pollution Prevention and Control Action Plan” was squarely on particulate matter. The plan mandated a nationwide reduction of annual average PM₁₀ concentrations by over 10% by 2017. For key regions like Beijing-Tianjin-Hebei, the Yangtze River Delta, and the Pearl River Delta, it set even stricter binding reduction targets for PM_{2.5} (25%, 20%, and 15%, respectively). These targets were cascaded down to local governments through assessment indicators, and their fulfillment was directly tied to local officials’ performance evaluations, promotions, and even political careers of local officials, effectively serving as a “one-vote veto” metric—meaning that failure on this single indicator could override positive performance across all other dimensions of cadre evaluation. In stark contrast, while the Action Plan mentioned ozone, it set no binding quantitative targets, nor was ozone integrated into the official evaluation system.

An Urban-Biased Monitoring and Accountability Network. Before 2013, China’s air quality monitoring network was sparse and often criticized for data manipulation (Ghanem and Zhang, 2014). To ensure authentic data for performance evaluations, the central gov-

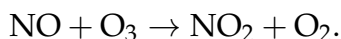
ernment established a vertically managed national monitoring network, implementing it in phases between 2013 and 2015. However, the spatial layout of these new monitoring stations was almost exclusively concentrated in the urban built-up areas of prefecture-level cities, leaving vast rural areas largely outside direct national oversight (see Appendix C for details).⁴ This institutional design incentivized rational local officials to focus their limited abatement resources on the heavily monitored urban centers, subjecting these areas to a more intense regulatory shock.

In summary, the institutional setting of our study is characterized by an environmental accountability system centered on PM_{2.5} and a monitoring network with a spatial bias toward urban areas. While effective in achieving its intended goal, this institutional design inadvertently gave rise to a series of unintended consequences.

2.2 The Mechanism: Incentives and Atmospheric Chemistry

China’s dramatic progress in reducing PM_{2.5} over the past decade has coincided with a troubling rise in ground-level ozone (O₃) concentrations. This asymmetric pollution trend is not merely a consequence of atmospheric dynamics but stems from the interaction between institutional incentives and nonlinear chemical responses. Specifically, the central government’s PM_{2.5}-centric accountability framework has systematically shaped local enforcement strategies in ways that unintentionally promote O₃ formation through two reinforcing pathways—one behavioral and one physicochemical.

Pathway I: Strategic Precursor Abatement and Behavioral Feedback. PM_{2.5} and O₃ originate partly from shared precursors, notably nitrogen oxides (NO_x) and volatile organic compounds (VOCs). However, their roles in O₃ formation differ markedly. NO_x contributes to O₃ photochemistry while simultaneously suppressing peak concentrations via the titration reaction:



In urban China, atmospheric chemistry typically resides in the VOC-limited regime, wherein O₃ formation rates are constrained more by VOC availability than by NO_x (Wang et al., 2019; Li et al., 2019). Consequently, disproportionate reductions in NO_x—relative to VOCs—

⁴According to our statistics, more than 94% of the monitoring stations are located in the built-up areas.

diminish the titration effect without correspondingly slowing photochemical activity, leading to elevated O₃ levels. Likewise, increases in VOCs under such conditions sharply accelerate O₃ production. Thus, any regulatory strategy that prioritizes NO_x abatement over VOC control—even if efficient for PM_{2.5} reduction—can inadvertently catalyze O₃ buildup.

Pathway II: Physicochemical Suppression via PM_{2.5} Scavenging. Beyond precursor interactions, PM_{2.5} itself exerts a direct inhibitory effect on O₃ formation. Fine particulate matter provides reactive surfaces that adsorb hydroperoxyl radicals (HO₂), key intermediates in tropospheric ozone synthesis. Reductions in PM_{2.5} therefore leave more HO₂ radicals available in the atmosphere, amplifying the photochemical production of O₃ (Li et al., 2019). While decreased PM_{2.5} may also enhance solar radiation and further stimulate O₃ formation, this radiative channel is quantitatively secondary to radical-mediated effects (Li et al., 2019; Le et al., 2020).

Institutional Origin of the Substitution Pattern. From an economic perspective, this chemically counterproductive abatement pattern arises endogenously from the incentive structure embedded in China's environmental governance. Local governments face binding PM_{2.5} targets and are evaluated based on urban air quality metrics. These institutional constraints induce rational, cost-minimizing responses. SO₂ stems largely from large point emission sources like coal-fired power plants, which are relatively easy to monitor and regulate. By contrast, NO_x and especially VOCs originate from dispersed and heterogeneous sources, including large point sources (which account for a very small fraction of VOC emissions) and diffuse sources such as small industries, vehicle exhaust, and solvent use—posing substantial enforcement challenges (Shao et al., 2009; Dallmann et al., 2012).⁵ Officials concentrate enforcement on large, stationary sources—such as coal-fired power plants—where SO₂ and NO_x abatement delivers rapid and measurable PM_{2.5} reductions. By contrast, controlling diffuse VOC sources (e.g., solvent use, vehicle evaporative emissions) requires substantially higher administrative and monitoring costs, with limited short-term impact on PM_{2.5} mass. As modeled in Appendix H, this enforcement asymmetry produces a decline in SO₂ and NO_x emissions, but an increase in VOC emissions. Simultaneously, enforcement resources are spatially skewed toward urban monitors, further exacerbating rural under-

⁵According to Zheng et al. (2021), in 2013, point emission sources accounted for 84% of SO₂ emissions, 58% of NO_x emissions, and 17% of VOC emissions in China.

regulation.

Implications. Together, these mechanisms establish a clear causal chain: institutional design shapes regulatory behavior, which in turn reshapes the composition of precursor emissions. The resulting pollutant substitution—favoring O₃-promoting emissions—is not a random outcome but a predictable response to misaligned incentives. Since O₃ inflicts broad ecological damage, particularly to vegetation and agricultural systems (Agathokleous et al., 2020, 2023), this shift may impose substantial unaccounted-for environmental costs, underscoring the importance of multi-pollutant policy frameworks.

2.3 Stylized Facts

We begin by examining the evolution of aggregate air pollution in China. Figure 1 illustrates our first key stylized fact: following the implementation of a PM_{2.5}-targeted environmental policy in 2013, the national average concentrations of PM_{2.5} and O₃ have diverged markedly. Prior to the policy, trends for both pollutants were relatively stable. After 2013, however, the PM_{2.5} index underwent a sharp and sustained decline, falling from 100 in 2013 to approximately 60 in 2019, a reduction of about 40%. In contrast, the ozone index increased from 100 to roughly 120, rising by over 20%. This diverging trajectory provides preliminary, descriptive support for a potential pollutant substitution effect.

Figure 2 further illustrates the changing gap in pollutant concentrations between high- and low-stringency areas. Panel A shows that after the policy intervention, the gap in PM_{2.5} concentration between the more intensely regulated urban areas and the less regulated rural areas narrowed, falling from over 17 $\mu\text{g m}^{-3}$ in 2013 to less than 10 $\mu\text{g m}^{-3}$ in 2019. Panel B, however, reveals the opposite trend for O₃: the urban–rural gap widened. This asymmetric trend suggests a critical unintended consequence: in the process of aggressively reducing PM_{2.5}, heavily scrutinized urban areas may have altered the atmospheric chemical balance in a way that fostered ozone generation. The phenomenon shown in this figure, where a policy aimed at improving air quality by controlling one pollutant exacerbates another, provides the key empirical context for our subsequent causal analysis.

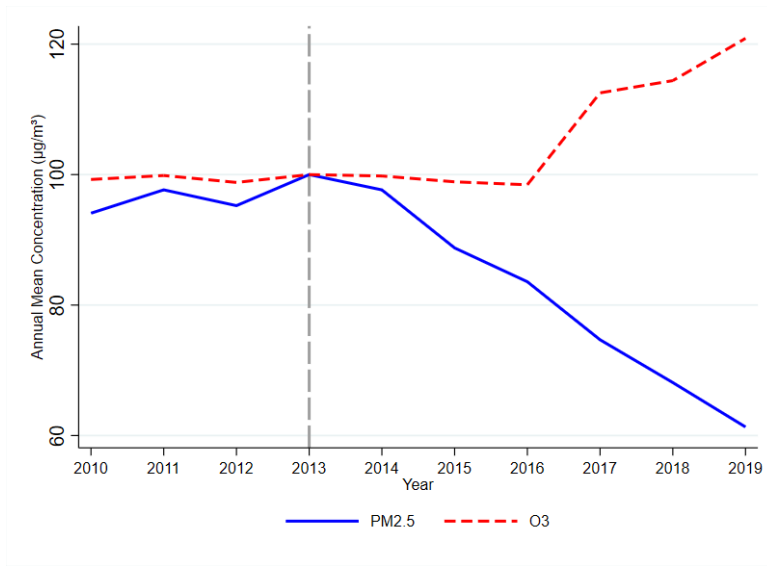
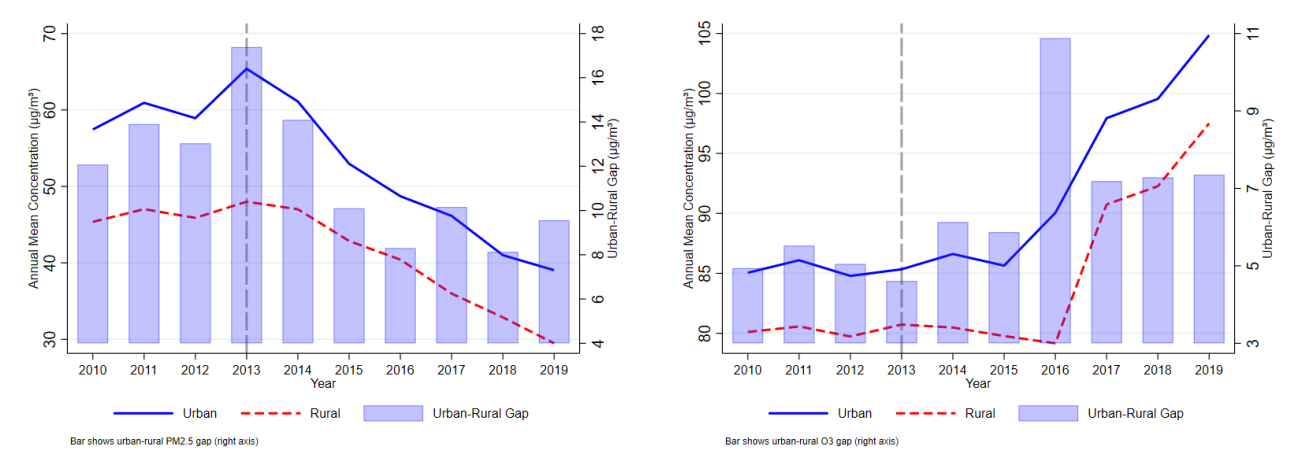


Figure 1: The “Great Divergence”: Contrasting Trends of PM_{2.5} and O₃ Concentrations in China

Note: This figure displays the average pollutant indices (normalized to 100 in 2013) for the period 2010–2019. The vertical dashed line indicates the 2013 launch of China’s “War on Pollution”. The sample includes 904,743 grid cells, consistent with the sample size used in the baseline regression. Grid-level pollutant concentrations are sourced from the CHAP dataset developed by Wei et al. (2021) and Wei et al. (2022).



(a) Urban-Rural PM_{2.5} Gap

(b) Urban-Rural O₃ Gap

Figure 2: Evolution of the Urban–Rural Pollutant Concentration Gap

Notes: This figure plots the annual trend in the level of pollutant concentrations and the urban–rural gap. The vertical dashed line marks the 2013 policy launch. Panel A shows the annual average PM_{2.5} concentrations in urban and rural areas and their gap, while Panel B shows the annual average O₃ concentrations in urban and rural areas and their gap. The sample contains 904,743 grids, consistent with the sample size in the baseline regression. Grid-level pollutant concentrations are from the CHAP dataset from Wei et al. (2023).

2.4 A Model of Pollutant Substitution

To formalize the incentive mechanism described above, we develop an equilibrium model featuring both firms and the local government as strategic agents (see Appendix H for the full derivation). Our model embeds the atmospheric chemistry relationships between precursor emissions, $PM_{2.5}$, and O_3 , into a principal–agent framework where a local government allocates finite enforcement resources across three precursor pollutants (SO_2 , NO_x , and VOCs) to minimize pollution damages, while firms choose abatement in response to enforcement intensity.

The model yields two key insights. First, under a $PM_{2.5}$ -focused accountability system, the regulator’s cost-minimizing strategy concentrates enforcement on precursors with the highest $PM_{2.5}$ return per regulatory dollar—primarily SO_2 and, to a lesser extent, NO_x —while diverting resources away from VOC sources. This enforcement reallocation, driven by the binding budget constraint, can cause VOC enforcement to *fall below* its pre-policy level, generating an increase in VOC emissions (Proposition 1 in Appendix H). Second, this asymmetric emission response—declining SO_2 and NO_x alongside rising VOCs—creates atmospheric conditions that promote O_3 formation through both the behavioral pathway (the altered precursor mix) and the physicochemical pathway ($PM_{2.5}$ reduction itself), leading to a simultaneous decline in $PM_{2.5}$ and rise in O_3 (Proposition 2 in Appendix H).

2.5 Hypotheses

Based on the institutional analysis, stylized facts, and theoretical model in Appendix H, we formulate the following hypotheses:

Hypothesis 1 (Pollutant Substitution): The $PM_{2.5}$ -focused accountability system incentivizes local governments to reallocate enforcement resources toward $PM_{2.5}$ precursors, leading to a significant decrease in $PM_{2.5}$ concentrations but a simultaneous increase in O_3 concentrations.

Hypothesis 2 (Accountability Pressure Amplifies Substitution): Cities facing stronger $PM_{2.5}$ accountability pressure exhibit both larger $PM_{2.5}$ reductions and larger O_3 increases, because greater pressure amplifies the enforcement reallocation mechanism.

Hypothesis 3 (Asymmetric Emission Mechanism): This pollutant substitution is driven

by asymmetric enforcement allocation under resource constraints: local governments concentrate their enforcement on SO₂ and NO_x (high PM_{2.5} return, low enforcement cost) while reducing enforcement on VOCs (low PM_{2.5} return, high enforcement cost), producing a sharp decline in SO₂ and NO_x emissions alongside an increase in VOC emissions.

Hypothesis 4 (Unintended Ecological Damage): Given the greater ecological threat posed by ozone, the substitution from PM_{2.5} to O₃ leads to a significant decline in local biodiversity, representing a substantial unintended cost of the policy.

3 Empirical Strategy and Data

3.1 Empirical Strategy

Our empirical analysis is based on a 0.1° × 0.1° (approximately 10 km × 10 km at China’s latitude) grid-level panel dataset covering mainland China from 2010 to 2019, comprising over 90,000 grid cells. A grid-level analysis offers two key advantages. First, it allows us to precisely capture the spatial heterogeneity of air pollution within administrative regions. Second, within a fixed-effects framework, it enables us to effectively control for time-invariant micro-geographical features such as topography and landforms that could otherwise confound the analysis.

Building on this panel, we leverage the staggered roll-out of the national air quality monitoring network as a quasi-natural experiment. We employ a staggered difference-in-differences (DID) design to test for differential changes in pollution between areas with high and low regulatory stringency. Existing research confirms that there are spatial disparities in the intensity of air pollution control efforts by local governments (Yang et al., 2024). Since the monitoring stations are overwhelmingly concentrated in urban areas, we define the more intensely regulated urban areas as the treatment group and the less regulated rural areas as the control group. This leads to the following specification:

$$y_{ict} = \alpha \text{treat}_i \times \text{post}_{ct} + \gamma^T X_{act} + D_i + D_{ct} + u_{ict}, \quad (1)$$

where the subscript i denotes a grid cell, c denotes the prefecture-level city to which grid

i belongs, t denotes the year, and a denotes the area (urban area or rural area) in which grid i is located. The outcome variable, y_{ict} , represents our variables of interest, primarily grid-level PM_{2.5} and O₃ concentrations. $treat_i$ is a dummy variable equal to 1 if grid cell i is located within an urban built-up area and 0 otherwise. $post_{ct}$ is a dummy variable that equals 1 for city c in all years after it was first integrated into the national air quality monitoring network and 0 otherwise. We add city-area-year level meteorological variables X_{act} to control for weather factors affecting pollutant concentrations. We also include grid fixed effects, D_i , to control for time-invariant characteristics such as location, elevation, and topography, and include city-year fixed effects, D_{ct} , to absorb any time-varying city level shocks, such as changes in local climate patterns, mayoral turnover, industrial policies, or macroeconomic trends. Standard errors are clustered at the grid level. The coefficient of interest is α , which captures the differential change in pollution in treatment areas relative to control areas following the policy implementation.

3.2 Data Sources and Variable Construction

We construct a comprehensive dataset combining environmental and ecological data from multiple sources. Appendix B provides further details on data construction, and Table A1 in Appendix A reports summary statistics for the main variables.

Core explanatory variables. *National Air Quality Monitoring Policy ($post_{ct}$):* We obtained the precise geographic locations of all national monitoring stations from the China National Real-time Air Quality Publishing Platform. By cross-referencing official announcements from the Ministry of Ecology and Environment, we compiled the specific year in which each prefecture-level city was first included in the national network.

Urban–Rural Division ($treat_i$): We use the Global Urban Boundary (GUB) dataset from Zhao et al. (2021) to define urban areas. Based on the 2012 built-up urban area boundaries, we identify whether each grid cell is located within an urban area.

Outcome variables. *Air Pollutant Concentrations:* We source annual average PM_{2.5} and O₃ concentration data for 2010–2019 from the China High Air Pollutants (CHAP) dataset, which

provides high-resolution, high-quality estimates.⁶ We calculate the average annual concentration for each grid cell with GIS software.

Pollution Emission Data: To investigate the policy's impact on precursor pollutants and discuss the potential mechanism of the pollution substitution phenomenon, we also use annual emissions data from the Multi-Resolution Emission Inventory for China (MEIC), developed by Tsinghua University to construct grid-level annual emissions for PM_{2.5}, SO₂, NO_x, and VOCs.⁷

Biodiversity: We use bird abundance and bird species richness as our primary proxies for biodiversity. The reasons for this choice are as follows. First, birds are widely recognized as valuable indicator species (Liang et al., 2020). Their population trends provide an early and measurable signal of environmental change, reflecting disturbances that may later manifest across a wider range of species (e.g., plants, soil organisms, and carnivores feeding on birds). This makes them a suitable proxy for detecting initial ecological impacts. Second, birds are an important part of the ecosystem, undertaking crucial functions such as preying on insects, spreading pollen and seeds, and forming a complete food chain (Li et al., 2023; Matthews et al., 2024). Therefore, bird diversity is an important indicator of ecological health. Third, directly measuring ecological health presents difficulties in data acquisition, while the platform we use for bird observation provides an excellent source for quantitative analysis. Specifically, the data come from the China Bird Report Center, a citizen-science platform with extensive geographic and species coverage, including observations from over 2,200 counties covering more than 90% of all bird species in China. As bird observations do not provide continuous spatial coverage, a grid-level analysis would result in a substantial loss of sample size. Therefore, for the biodiversity analysis, our unit of observation is aggregated to the city–area (urban/rural)–year level. Appendix E provides details on the construction of the bird abundance and bird species richness measures.

Control variables: Meteorological control variables come from Qin and Zhang (2022),

⁶The PM_{2.5} and O₃ concentration data from CHAP dataset was developed by Wei et al. (2021) and Wei et al. (2022). Compared to previous satellite-based pollution data, it has higher resolution and higher prediction accuracy (the overall R-squared is 0.88 for PM_{2.5} model and 0.87 for O₃ model), providing an accurate data basis for our analysis.

⁷The website for the MEIC dataset is <http://meicmodel.org.cn>. It provides a high-resolution global multi-scale anthropogenic greenhouse gas and air pollutant emission inventory database. Li et al. (2017) and Zheng et al. (2018) introduce the construction method and present descriptive characteristics of the MEIC data.

a high-resolution (1 day, 1 km) gridded dataset for temperature and precipitation across China. We aggregate the data to the city-area-year level.

4 Pollutant Substitution and Its Mechanisms

4.1 Baseline Results

Panel A in Table 1 presents the baseline results from estimating Equation (1). Columns (1)–(3) examine the policy’s impact on $\text{PM}_{2.5}$ concentrations. Across specifications with increasingly stringent fixed effects and control variables, the interaction coefficient is consistently negative and statistically significant at the 1% level. In our preferred and most demanding specification, shown in Column (3), the coefficient is -0.573 , indicating that following the policy’s implementation, $\text{PM}_{2.5}$ concentrations in urban areas decreased by approximately $0.573 \mu\text{g m}^{-3}$ relative to rural areas. Columns (4)–(6) of Table 1 report the results for ozone concentrations. The estimated coefficient on the interaction term is positive and statistically significant in all specifications. Our most credible specification, shown in Column (6), implies that the policy led to a significant increase in O_3 concentrations of about $0.560 \mu\text{g m}^{-3}$ in treatment areas compared to the control areas.

To address potential biases inherent in the traditional fixed effects estimator under a staggered DID design, we apply the heterogeneity-robust DID approach developed by [Cengiz et al. \(2019\)](#) to assess our baseline findings. As reported in Panel B, the estimates align closely with those in Panel A in terms of both statistical significance and direction, and the estimated magnitudes remain comparable. These results, presented in Table 1, lend support to Hypothesis 1: while the $\text{PM}_{2.5}$ -targeted environmental policy effectively achieved its primary objective, it concurrently triggered a structural reallocation across pollutants, resulting in an unintended rise in ozone concentrations.

4.2 Dynamic Effects

To validate our research design and examine the dynamics of the policy’s impact, we conduct an event study analysis. We replace the interaction term in our main specification with

Table 1: Impact of Monitoring Policy on PM_{2.5} and O₃

	(1)	(2)	(3)	(4)	(5)	(6)
	PM _{2.5}			O ₃		
Panel A: TWFE Model						
treat × post	-1.391*** (0.056)	-1.416*** (0.056)	-0.573*** (0.029)	0.938*** (0.051)	0.918*** (0.051)	0.560*** (0.033)
post	0.908*** (0.028)	0.933*** (0.027)		-0.630*** (0.029)	-0.668*** (0.029)	
Observations	904,743	904,743	904,743	904,743	904,743	904,743
R-squared	0.976	0.976	0.988	0.927	0.928	0.962
Panel B: Heterogeneity-Robust DID Method from Cengiz et al. (2019)						
ATT	-1.820*** (0.064)	-1.825*** (0.065)	-0.991*** (0.110)	1.094*** (0.055)	1.076*** (0.055)	0.790*** (0.090)
Controls	No	Yes	Yes	No	Yes	Yes
Grid FE	Yes	Yes	Yes	Yes	Yes	Yes
Province-Year FE	Yes	Yes	No	Yes	Yes	No
City-Year FE	No	No	Yes	No	No	Yes

Notes: This table reports the results for the impact of the target-based environmental regulation policy on pollutant concentrations. Panel A uses TWFE models with interactive fixed effects and Panel B uses a heterogeneity-robust DID method from [Cengiz et al. \(2019\)](#) to alleviate the heterogeneous treatment bias. All the columns control grid fixed effects. Meteorological control variables are controlled in Columns (2), (3), (5), and (6). Columns (1), (2), (4), and (5) control the province-year fixed effects, while Columns (3) and (6) control the city-year fixed effects. Standard errors, clustered at the grid level, are in parentheses. * $p < 0.10$, ** $p < 0.05$, *** $p < 0.01$.

a series of interactions between the treatment indicator and year dummies relative to the policy's initiation:

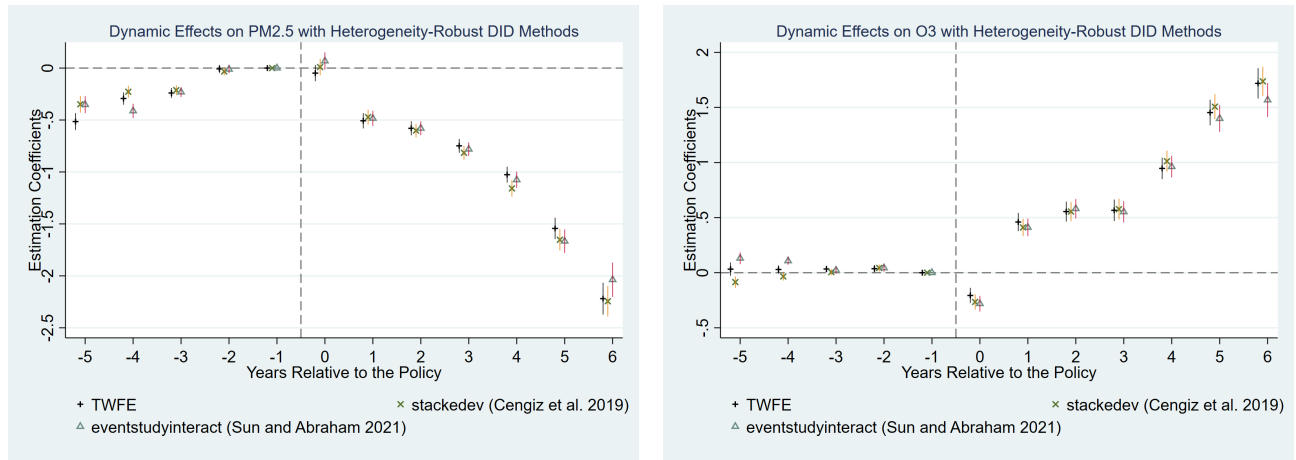
$$y_{ict} = \sum_{k=-5}^6 \beta_k D_{ct}^k \cdot \text{treat}_i + \gamma X_{act} + D_i + D_{ct} + u_{ict}, \quad (2)$$

where D_{ct}^k is a dummy variable for the k -th year relative to the policy roll-out in city c . For example, D_{ct}^{-1} equals one for the year just before the policy was implemented. We use the year before implementation as the omitted base period. D_{ct} captures the city-year fixed effects. Figure 3 plots the estimated coefficients β_k and their 90% confidence intervals. We also use two heterogeneity-robust DID methods from [Cengiz et al. \(2019\)](#) and [Sun and Abraham \(2021\)](#) to assess the baseline fixed effect model.

Figure 3 illustrates the contrasting dynamic responses of PM_{2.5} and O₃ concentrations

to the policy. In Figure 3a, the coefficient estimates—capturing the differential trend between treatment and control groups—drift upward prior to implementation, suggesting a narrowing gap in $PM_{2.5}$ levels. Once the policy is enacted, this trend reverses sharply: the coefficient declines monotonically from near zero to approximately -2.25, with growing magnitude and statistical significance, indicating a marked reduction in particulate matter. In contrast, Figure 3b shows that O_3 concentration differentials hover around zero before the policy, but post-implementation they increase substantially from about -0.25 to 1.75, remaining elevated thereafter. This evidence points to a persistent and significant rise in ozone levels in treated areas, highlighting a clear policy-induced substitution between $PM_{2.5}$ and O_3 .

In summary, Figure 3, simultaneously validates the robustness of our research design and visualizes the core narrative of our paper: a successful $PM_{2.5}$ abatement policy was accompanied by a worsening O_3 problem. This provides a solid dynamic foundation for our subsequent analysis of the pollutant substitution mechanism.



(a) Dynamic Effects on $PM_{2.5}$ Concentrations

(b) Dynamic Effects on O_3 Concentrations

Figure 3: Dynamic Effects on the Pollutant Concentrations

Notes: This figure demonstrates the dynamic effects on pollutant concentrations using different models. The dots represent point estimates and the vertical lines represent 90% confidence intervals. All models include meteorological control variables, grid fixed effects, and city-year fixed effects. Standard errors are clustered at the grid-cell level. The year prior to the policy ($k = -1$) is the omitted base category.

4.3 Robustness Checks

In this subsection, we conduct a series of robustness checks to address various empirical challenges and rule out other possible confounding variables.

4.3.1 Regulatory Spillover Concerns

A key identification concern in our setting is the potential for regulatory spillovers. Specifically, due to the regional transport of pollutants, if local governments respond to the policy by extending controls into rural areas to further reduce urban pollution, our baseline estimates may be biased. To address this, we restrict the control group to rural grids located downwind of urban areas within the same city. Since air pollution flows primarily from upwind to downwind areas, emissions from these rural grids hardly affect urban air quality, thereby removing incentives for local officials to regulate them. As reported in Table 2, the resulting estimates are similar to those in Table 1, both in terms of statistical significance and magnitudes. This consistency supports the robustness of our baseline findings.

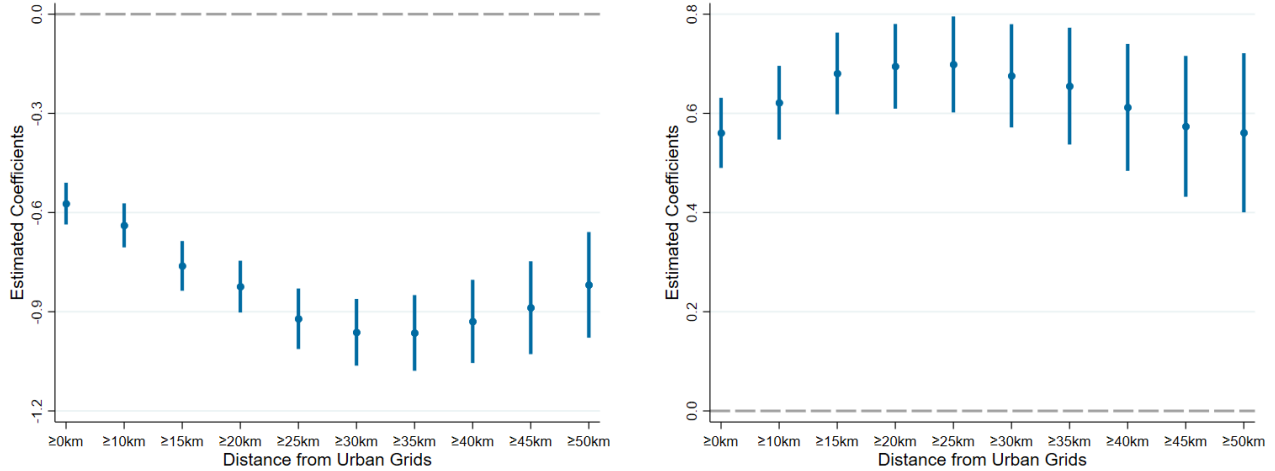
Table 2: Alleviating Spillover Concerns: Downwind Rural Grids as Control Group

	(1)	(2)	(3)	(4)	(5)	(6)
	PM _{2.5}			O ₃		
treat × post	-1.445*** (0.056)	-1.475*** (0.056)	-0.565*** (0.032)	0.994*** (0.052)	0.991*** (0.052)	0.555*** (0.036)
post	0.982*** (0.032)	1.008*** (0.031)		-0.583*** (0.035)	-0.653*** (0.035)	
Controls	No	Yes	Yes	No	Yes	Yes
Grid FE	Yes	Yes	Yes	Yes	Yes	Yes
Province-Year FE	Yes	Yes	No	Yes	Yes	No
City-Year FE	No	No	Yes	No	No	Yes
Observations	660,272	660,272	660,272	660,272	660,272	660,272
R-squared	0.974	0.974	0.987	0.920	0.922	0.962

Notes: This table reports the results that include all urban grids and rural grids located downwind of the urban grids. To alleviate the endogeneity concern caused by the spillover of government regulation, only the rural grids located downwind of the urban grids in their respective cities served as the control group. All columns control grid fixed effects. Meteorological control variables are controlled in Columns (2), (3), (5), and (6). Columns (1), (2), (4), and (5) control the province-year fixed effects while Columns (3) and (6) control the city-year fixed effects. Standard errors, clustered at the grid level, are in parentheses. * $p < 0.10$, ** $p < 0.05$, *** $p < 0.01$.

To further tighten the identification, we exploit variation in the distance between urban

and downwind rural grids. By incrementally increasing the minimum allowable distance from the urban areas, we progressively exclude rural grids that could plausibly be influenced by spillover motives. As illustrated in Figure 4, the estimated coefficients exhibit only minor fluctuations across distance bins, remaining stable in magnitude and statistical significance. This stability confirms that the baseline results are not driven by potential spillovers arising from proximity-based regulatory extensions.



(a) Effects on PM_{2.5} Concentration

(b) Effects on O₃ Concentration

Figure 4: Alleviating Spillover Concerns: Restricting the Scope of Control Grids

Notes: This figure demonstrates how estimated coefficients change as the distance between rural and urban grids increases. All regressions only include rural grids located downwind of urban grids in the same city as the control group. The horizontal axis represents the distance (km) between the downwind rural grid and the urban grid within the same city. The dots and the vertical lines represent the estimation coefficients and 95% confidence intervals. All specifications control for meteorological control variables, city-year fixed effects, and grid fixed effects. Standard errors are clustered at the grid level.

4.3.2 The Geographical Scale of Policy Effects

To examine the spatial reach of the PM_{2.5}-targeted monitoring policy and its implications for pollution substitution, we conduct a concentric ring analysis. Specifically, we replace the binary treatment indicator $treat_i$ in Equation (1) with a series of distance-bin indicators, partitioning rural grids into rings at 0–10 km, 10–15 km, and continuing in steps to more than 50 km from the nearest urban grid.

The results are shown in Figure A1. The reference category includes all urban grids. The estimated coefficients for each distance bin capture the differential effect of the urban-biased

policy on pollution concentrations in rural areas relative to urban areas. In Figure A1a, all coefficients are positive and statistically significant, indicating that the policy is associated with larger reductions in $PM_{2.5}$ concentrations in urban areas. The effect diminishes with distance, before rebounding in the outermost bin beyond 50 km. Conversely, Figure A1b shows uniformly negative and significant coefficients, implying relatively larger increases in O_3 concentrations in urban areas. This effect also attenuates with distance, reversing beyond 50 km. Collectively, these patterns highlight a clear spatial gradient in the policy's heterogeneous impact on pollution concentrations, where the effect first intensifies and then weakens with the distance from the urban grid.

4.3.3 City Assignment to Monitoring Roll-out Waves

The assignment of cities to different monitoring roll-out waves is not random; it exhibits certain characteristics that have been comprehensively studied in recent literature (Greenstone et al., 2022; Barwick et al., 2024; Yang et al., 2024). We can summarize these characteristics as follows. First, the roll-out wave assignment mainly corresponds to administrative hierarchies that were determined long before the policy, with a few exceptions due to exogenous factors such as geographic contiguity. Second, cities in earlier waves tend to have a larger population, higher income, and higher levels of $PM_{2.5}$ pollution. Third, conditional on the predetermined administrative hierarchies and status, levels and trends in cities' pre-policy air pollution or income provide little to no additional explanatory power for city wave assignment. These characteristics do not threaten our identification since we add grid fixed effects that absorb the administrative hierarchies and locations of each city. Moreover, our baseline model includes city-year fixed effects that control for all unobservable factors at the city level that vary across years. In addition, we augment our model with interactions between year dummies and city level baseline (year 2010) characteristics, including $PM_{2.5}$ concentration, GDP per capita, administrative area, and urban populations. The results are shown in Table A4, Columns (1) and (2), which are consistent with our baseline model.

4.3.4 Placebo Tests

We also conduct placebo tests to verify our baseline results. We randomly assign treatment grids and randomly generate policy timing within the sample period for each city, while keeping the mean value of variables *treat* and *post* in the research sample unchanged. The DID estimation in Equation (1) is repeated 2000 times in each test. We plot the kernel density of placebo estimates and benchmark estimates in Figure A2a and A2b. The placebo estimates all follow an approximately standard normal distribution, with the benchmark coefficients (-0.573 and 0.560) lying outside the 99% confidence intervals, which verifies the robustness of our baseline results.

4.3.5 Alternative Measures of the Treatment Group

Our baseline analysis defines treatment areas as all built-up areas within a city's jurisdiction. As a stricter alternative, we redefine the treatment group to include only the built-up areas of the central municipal district, where monitoring stations are most concentrated. As shown in Appendix Table A2, Columns (1) and (2), the estimated effects remain highly significant, with an even larger reduction in PM_{2.5} (-0.961) and increase in O₃ (0.748).

4.3.6 Sensitivity Analyses on Sample Selection

To rule out the influence of outliers, we exclude Tibet and Xinjiang, two large western provinces with unique geographic and economic characteristics. The results (Table A2, Columns (3) and (4)) are nearly identical to our baseline estimates. We also extend our sample period to 2000–2019 to examine the policy's effects over a longer time horizon. The results (Table A2, Columns (5) and (6)) remain consistent with our baseline findings.

4.3.7 Interference from Other Concurrent Policies

While our city-by-year fixed effects control for all city-level homogeneous policies, a potential threat is a concurrent environmental policy implemented heterogeneously within cities (e.g., at the county level). The most relevant policy enacted during our study period is the

National Key Ecological Functional Zones program.⁸ We explicitly control for the designation of these zones in our regression. As shown in Table A4, Columns (3) and (4), the magnitude and significance of our main coefficients of interest remain unchanged, confirming that our results are not driven by this concurrent policy.

4.3.8 Analysis with Aggregated Data and Alternative Clustering Level

To provide an empirical basis for the biodiversity analysis in Section 5 and test the sensitivity to the spatial unit of analysis, we aggregate our data from the $0.1^\circ \times 0.1^\circ$ grid level to the city-area level and replicate the baseline results. The results, reported in Table A3, reconfirm our main findings, demonstrating that our conclusions are not contingent on a specific spatial scale. Moreover, we also replicate our baseline results with standard errors clustered at the prefecture city level to restrict the assumptions regarding error correlation. As shown in Table A5, the point estimates retain the same levels of statistical significance as in the baseline, further supporting the robustness of our results.

4.4 Mechanism Analysis

4.4.1 The Role of Environmental Accountability Pressure

Our baseline results establish the existence of pollutant substitution. A key question is whether the intensity of this effect varies with the degree of environmental pressure faced by local governments. We hypothesize that cities under greater pressure to perform will exhibit a stronger policy response. We test this using a DDD framework, interacting our baseline DID term with two proxies for pre-policy accountability pressure:

Pre-existing Pollution Level ($PM_{2.5_1012}$): The city's average $PM_{2.5}$ concentration in urban areas from 2010–2012. Cities with higher historical pollution burdens faced greater pressure to reduce emissions.

Pre-existing Non-Compliance Status ($PM_{2.5_ncc_d}$): A dummy equal to 1 if the city's

⁸The National Key Ecological Functional Zones program is a policy established by China's central government at the county level in batches in 2011 and 2017. At present, 676 county-level administrative regions have been included in the program, covering approximately 53% of China's land area. The aim is to promote green development and protect biodiversity through measures such as restricting large-scale industrialization and urbanization development and fiscal transfer payments.

urban PM_{2.5} concentration in 2012 exceeded the national standard of 35 $\mu\text{g m}^{-3}$. These “non-compliant” cities faced more intense scrutiny from both the central government and the public.

Columns (1), (2), (4), and (5) in Table 3 report the results. In Columns (1)–(2), all triple-interaction terms are significantly negative. In Columns (4)–(5), they are significantly positive. These results are unequivocal: cities facing greater pre-existing accountability pressure for PM_{2.5} experienced a significantly larger reduction in PM_{2.5} in their treatment areas, but also a significantly larger increase in O₃. This demonstrates that accountability pressure exacerbated the pollutant substitution effect, providing support for Hypothesis 2 by clearly linking assessment pressure to the pollution outcome.

4.4.2 The Role of Government Attention

While external pressure is a key driver, a local government’s own political will or attention can also shape policy implementation. We proxy for these internal policy priorities using textual analysis of annual municipal government work reports. We construct an index, PM_fre, which measures the frequency of keywords related to the air pollutant—particulate matter—in each city’s annual report.⁹

Columns (3) and (6) in Table 3 present the DDD results interacting our policy term with this attention index. The triple-interaction term in Column (3) is significantly negative, indicating that cities that paid more textual attention to particulate matter achieved greater PM_{2.5} reductions. The coefficient in Column (6) is significantly positive, showing that this heightened focus on PM_{2.5} was also associated with a larger increase in O₃. This provides complementary evidence for Hypothesis 2 from the perspective of revealed government priorities.

4.4.3 Direct Evidence: Impact on Anthropogenic Emissions

The preceding analyses show that pressure and attention matter. But what specific actions did they induce? To provide more direct evidence on the mechanisms involved, we use the MEIC dataset to examine the policy’s impact on the anthropogenic emissions of four key

⁹The phrases include (“PM₁₀”, “PM_{2.5}”, and “particulate matter” in Chinese).

Table 3: Mechanism Analysis: The Role of Environmental Accountability Pressure and Government Attention

	(1)	(2)	(3)	(4)	(5)	(6)
	PM _{2.5}			O ₃		
treat × post × PM _{2.5_1012}	-0.570*** (0.167)			0.699** (0.304)		
treat × post × PM _{2.5_ncc_d}		-0.215*** (0.073)			0.412* (0.248)	
treat × post × PM_fre			-2.465*** (0.282)			2.333*** (0.327)
treat × post	-0.283*** (0.079)	-0.376*** (0.065)	-0.488*** (0.031)	0.204 (0.172)	0.184 (0.232)	0.402*** (0.033)
Controls	Yes	Yes	Yes	Yes	Yes	Yes
City-Year FE	Yes	Yes	Yes	Yes	Yes	Yes
Grid FE	Yes	Yes	Yes	Yes	Yes	Yes
Observations	842,593	842,593	477,411	842,593	842,593	477,411
R-squared	0.988	0.988	0.993	0.958	0.958	0.981

Notes: This table examines the moderating role of environmental accountability pressure and government attention. The dependent variables are PM_{2.5} in Columns (1)–(3) and O₃ (Columns (4)–(6)) concentrations. All models include meteorological control variables, grid fixed effects, and city-year fixed effects. *PM_{2.5_1012}* is the average urban PM_{2.5} concentration from 2010–2012. *PM_{2.5_ncc_d}* is a dummy for cities exceeding the national PM_{2.5} standard in 2012. *PM_fre* is the frequency of particulate-matter-related keywords in the city’s annual government work report. We normalized *PM_{2.5_1012}* and *PM_fre* to the range [0, 1] using min-max normalization before adding them to the regression equation. Standard errors, clustered at the grid level, are in parentheses. **p*<0.10, ***p*<0.05, ****p*<0.01.

pollutants: PM_{2.5}, SO₂, NO_x, and VOCs.

Table 4 reveals that the PM-targeted policy achieved its primary objectives with notable success. Post-implementation, emissions of PM_{2.5} and SO₂ declined significantly by 8.5% and 20.7%, respectively — both pollutants being central to PM reduction. However, the policy exhibited asymmetric effects on other pollutant emissions. Column (3) shows no statistically significant change in NO_x emissions, while Column (4) documents a substantial 13.5% increase in VOC emissions. More importantly, Column (5) indicates that the policy significantly altered the relative emissions of VOCs to NO_x, creating conditions conducive to tropospheric O₃ formation.

These asymmetric effects arise from fundamental differences in the emission source characteristics. SO₂ primarily originates from large, centralized point sources (Smith et al., 2011), which are comparatively easier to monitor and regulate. In contrast, NO_x and particularly VOCs stem from a more complex mix of sources: not only large point sources, but also numerous and spatially dispersed sources such as small-scale industrial facilities, vehicle

exhaust emissions, and solvent utilization (Shao et al., 2009; Dallmann et al., 2012). These latter sources present greater challenges for monitoring, enforcement, and cost-effective control due to their diffuse nature.¹⁰ The null effect on NO_x may reflect the fact that emission reductions from large industrial sources were offset by increases from under-regulated sectors such as transportation. The sharp rise in VOC emissions suggests that the policy may have failed to address the dispersed sources, which have unintentionally created a favorable condition for VOC-intensive activities, or at the very least, did not effectively restrain their growth. Moreover, the findings are consistent with existing scientific research such as Zheng et al. (2018), who found that emissions of PM_{2.5} SO₂ declined while emissions of VOCs rose, relative to those of NO_x, after China's "War on Pollution".

In other words, while the policy successfully reduced the emissions of targeted pollutants, it substantially altered the atmospheric precursor mix by increasing VOC emissions and maintaining high NO_x levels. This shift generated "high-NO_x, high-VOCs" conditions, scientifically recognized as drivers of surface O₃ formation. These asymmetric adjustment in emissions reflects that a regulator facing a binding enforcement budget strategically re-allocates effort toward easily controlled precursors like SO₂, while neglecting more diffuse ones like VOCs. Thus, single-pollutant regulatory targets can induce unintended chemical equilibrium with adverse environmental consequences. The results provide empirical evidence for Hypothesis 3.

4.4.4 Separation of Two Scientific Pathways for O₃ Deterioration

The above results demonstrate that the substitution between PM_{2.5} and O₃ is an interplay of political incentives and scientific principles. We have introduced two different scientific pathways in Section 2.2, but we have not yet quantitatively separated their effects. Such separation is both important and interesting because each pathway has different policy implications. The first pathway reflects O₃ deterioration due to improper management of precursor pollutants (the behavioral pathway). The second pathway reflects O₃ deterioration directly caused by the policy-induced declines in PM_{2.5} (the physicochemical pathway). Specifically,

¹⁰In a 2022 interview, officials from the Ministry of Ecology and Environment pointed out that when treating VOCs in the past, China encountered problems such as inadequate source control, pollution control, standardized management, and insufficient regulatory capacity. (<https://eco.cctv.com/2022/11/05/ARTIJKhpwfpfJq22jMryb3mH221105.shtml>)

Table 4: Direct Evidence: Impact on Anthropogenic Emissions

	(1)	(2)	(3)	(4)	(5)
	ln(PM _{2.5})	ln(SO ₂)	ln(NO _x)	ln(VOCs)	ln($\frac{\text{VOCs}}{\text{NO}_x}$)
treat × post	-0.085*** (0.008)	-0.207*** (0.012)	-0.013 (0.009)	0.135*** (0.004)	0.147*** (0.009)
Controls	No	No	No	No	No
City-Year FE	Yes	Yes	Yes	Yes	Yes
Grid FE	Yes	Yes	Yes	Yes	Yes
Observations	148,720	148,720	148,720	148,720	146,690
R-squared	0.997	0.995	0.997	0.999	0.956

Notes: This table examines the policy’s impact on anthropogenic emissions. The dependent variables in Columns (1)–(5) are the natural logs of emissions for PM_{2.5}, SO₂, NO_x, VOCs, and $\frac{\text{VOCs}}{\text{NO}_x}$, respectively. Due to the limitation of MEIC resolution, we conduct the analysis at the 0.25° × 0.25° grid. All models include grid fixed effects and city-year fixed effects. Meteorological controls are not included because emissions are anthropogenic and not weather-dependent at the annual level. Standard errors are clustered at the grid level. * $p < 0.10$, ** $p < 0.05$, *** $p < 0.01$.

the behavioral pathway indicates that the reverse changes of VOCs and NO_x induced by local governments will worsen O₃ pollution. However, the physicochemical pathway reveals that even if the influence of VOCs and NO_x is excluded, the decline of PM_{2.5} itself will worsen O₃ pollution through a series of physicochemical mechanisms.

We utilize a simple approach, briefly described here and detailed in Appendix D, to quantitatively separate these two pathways. The goal of this framework is to separate the influence of NO_x and VOCs (the common precursor pollutants of O₃ and PM_{2.5}) on O₃ and the influence of PM_{2.5} itself on O₃. First, we regress the PM_{2.5} concentration on all its precursor pollutants, including SO₂, NO_x, and VOCs. Then, we obtain the predicted value of PM_{2.5} after eliminating the influences of NO_x and VOCs ($\widehat{PM}_{2.5}$) from the regression result. $\widehat{PM}_{2.5}$ represents the change in PM_{2.5} driven by SO₂ (SO₂ is only a precursor pollutant for PM_{2.5}, not for O₃). Finally, we regress O₃ on $\widehat{PM}_{2.5}$ and its precursor pollutants.¹¹ The coefficient of $\widehat{PM}_{2.5}$ reflects the physicochemical relationship between PM_{2.5} and O₃.

The results in Table A6 show that when excluding the effects of NO_x and VOCs, a 1 μg m⁻³ decrease in PM_{2.5} concentration is associated with approximately a 0.721 μg m⁻³ increase in O₃ concentration, on average, which reveals the physicochemical relationship.

¹¹To capture the nonlinear relationship between the precursor pollutants NO_x and VOCs and the secondary pollutants PM_{2.5} and O₃, we include the squared terms and interaction terms of these two precursor pollutants in the regressions. All regressions include meteorological control variables.

Combining this estimate with the baseline results in Table 1, we can briefly calculate that the physicochemical pathway (the second pathway) accounts for approximately 73.8% of the effect, while the remaining 26.2% is attributable to the imbalanced abatement of NO_x and VOCs.¹² These separation results here are consistent with Li et al. (2019), which suggests that the physicochemical relationship between PM_{2.5} and O₃ is the primary driver of the rising O₃ trend in the North China Plain during the “War on Pollution”. They further reveal the limitations of PM-targeted environmental policy. On one hand, achieving the PM_{2.5} target itself induces O₃ increases to some extent. On the other hand, the strategic regulations of local governments (as shown in Table 4) further exacerbate O₃ pollution. Therefore, while controlling PM_{2.5} concentrations, governments must incorporate multiple pollutants into their evaluation frameworks and take more forceful measures to control VOCs and NO_x, in order to achieve an overall improvement in air quality.

5 Ecological Consequences: The Impact on Biodiversity

The preceding sections have documented the phenomenon of pollutant substitution and its underlying mechanisms. Yet a critical question remains unaddressed: do these unintended shifts in pollutant composition impose tangible, quantifiable social costs through their ecological impacts? While scientific consensus recognizes O₃ as a more potent threat to ecosystems than PM_{2.5}, the economic literature has yet to rigorously quantify how such pollution substitution affects biodiversity. This section bridges that gap by examining the ecological consequences of pollutant changes, focusing on biodiversity as a core dimension of environmental and social welfare.

We use bird diversity—measured by bird abundance and bird species richness—as our primary proxy for ecological health. This approach offers several advantages. First, birds are widely recognized as valuable indicator species (Liang et al., 2020). Their population trends provide an early and measurable signal of environmental change, reflecting disturbances that may later manifest across a wider range of species. Moreover, bird observation data offer three critical advantages for our quantitative analysis: high temporal resolution,

¹² $\frac{-0.573 \mu\text{g m}^{-3} \times -0.721}{0.560 \mu\text{g m}^{-3}} \approx 0.738$

extensive spatial coverage, and broad taxonomic representation—features that collectively bolster the robustness and validity of our findings. To demonstrate a more general ecological impact on biodiversity, we also employ the Biodiversity Intactness Index (BII) created by the Natural History Museum, London as an alternative measure. Appendix E presents more details about the construction of bird diversity indicators, and Appendix F does the same for the identification strategy. Appendix G provides detailed information about general biodiversity analysis.

5.1 The Impact of Monitoring Policy on Bird Diversity

We first test the overall impact of the policy on biodiversity from the perspective of bird diversity. Table 5 reports the results. Our coefficient of interest, the interaction term, captures the differential change in bird abundance and bird species richness between the treatment and control areas after the policy. In Columns (1)–(3), the coefficient is significantly negative at the 1% level, regardless of the combination of control variables. This indicates that the implementation of the policy led to a significant decline in bird abundance in the more intensely regulated areas relative to the less regulated areas. Columns (4)–(6) show that the coefficient is likewise significantly negative for bird species richness. We also apply the heterogeneity-robust DID approach developed by Cengiz et al. (2019) to assess the fixed effect model findings. As reported in Panel B, the estimates align closely with those in Panel A in terms of both statistical significance and direction, and the estimated magnitudes remain comparable.

The results in Table 5 suggest that the target-based environmental policy not only reconfigured the structure of pollution but also generated a severe unintended ecological consequence: areas with stricter PM_{2.5} regulation experienced a significant deterioration in biodiversity. This provides initial support for Hypothesis 4.

Figure 5 shows the dynamic effects of the urban-biased monitoring policy on bird abundance and bird species richness. In addition to the traditional fixed effects model, we also use two heterogeneity-robust DID methods from Cengiz et al. (2019) and Sun and Abraham (2021). Prior to policy implementation, there were no significant differences in either bird abundance or species richness between urban and rural areas. Following the introduction of

Table 5: The Impact of Monitoring Policy on Bird Diversity

	(1)	(2)	(3)	(4)	(5)	(6)
	Bird Abundance			Bird Species Richness		
Panel A: TWFE Model						
treat×post	-0.337*** (0.104)	-0.330*** (0.104)	-0.340*** (0.114)	-0.122** (0.055)	-0.122** (0.056)	-0.140** (0.059)
post	0.078 (0.123)	0.073 (0.123)		0.001 (0.084)	0.004 (0.084)	
Observations	2,330	2,330	1,194	2,330	2,330	1,194
R-squared	0.580	0.580	0.796	0.561	0.562	0.805
Panel B: Heterogeneity-Robust DID Method from Cengiz et al. (2019)						
ATT	-0.305** (0.144)	-0.300** (0.144)	-0.391** (0.156)	-0.142* (0.082)	-0.141* (0.082)	-0.175** (0.079)
Controls	No	Yes	Yes	No	Yes	Yes
City-Area FE	Yes	Yes	Yes	Yes	Yes	Yes
Province-Year FE	Yes	Yes	No	Yes	Yes	No
City-Year FE	No	No	Yes	No	No	Yes

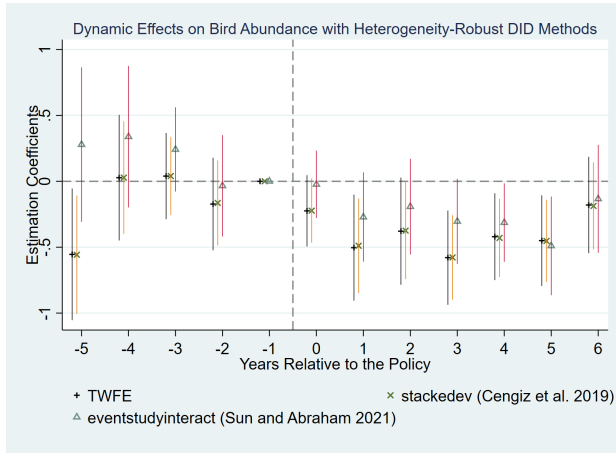
Notes: This table reports the DID estimates for the impact of the target-based environmental regulations on bird diversity. The dependent variable is bird abundance in Columns (1)–(3) and bird species richness in Columns (4)–(6). Panel A uses TWFE models with interactive fixed effects and Panel B uses heterogeneity-robust DID method from [Cengiz et al. \(2019\)](#) to alleviate the heterogeneous treatment problems. All columns include city-area fixed effects. Columns (2), (3), (4), and (5) include meteorological controls. Columns (1), (2), (4), and (5) control province-year fixed effects, while Columns (3) and (6) include city-year fixed effects. Standard errors are clustered at the city-area level. * $p < 0.10$, ** $p < 0.05$, *** $p < 0.01$.

the policy, the estimated coefficients declined markedly and remained significantly negative for most post-treatment periods. Although the magnitude of the coefficients exhibits some attenuation in later years, the overall trajectory continues to trend downward relative to the pre-policy baseline.

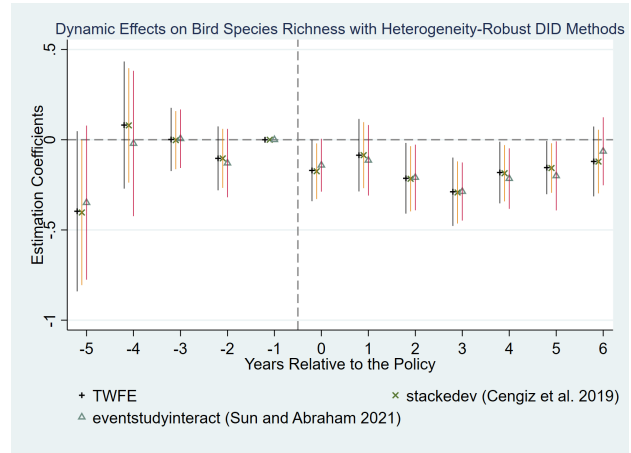
We also conduct placebo tests for the results shown in Table 5, using the same methods as those in Section 4.3. The results are plotted in Figure A2c and A2d. The red lines, indicating the baseline estimated coefficients, lie outside the 90% confidence intervals of the placebo estimator distributions, which verifies the robustness of the results shown in Table 5.

5.2 Pollutant Substitution as the Mechanism for Bird Diversity Loss

Having established the policy’s negative effect on bird diversity, we now test whether this is driven by the pollutant substitution phenomenon. To formally link the channels, we fol-



(a) Dynamic Effects on Bird Abundance



(b) Dynamic Effects on Bird Species Richness

Figure 5: Dynamic Effects on Bird Diversity

Notes: This figure reports the dynamic effects on bird diversity with different models. The plotted estimates are the estimated coefficients with 90% confidence intervals. All models control for the meteorological variables, city-area fixed effects, and city-year fixed effects. Standard errors are clustered at the city-area level.

lowing [Bertrand and Mullainathan \(2001\)](#) to employ a two-stage analytical framework (see [Appendix F](#) for details). Since [Liang et al. \(2020\)](#) document that O_3 has a significantly negative impact on bird populations while $PM_{2.5}$ does not, we only focus on O_3 here. In the first stage, we predict the policy-induced changes in O_3 concentrations. This regression helps isolate the effects of monitoring policy shocks on O_3 concentrations. In the second stage, we regress the bird diversity measures on the predicted O_3 concentration from the first stage with the same controls and fixed effects used in the first stage. The second-stage regression coefficient captures the effects of monitoring policy easing on bird diversity through the pollution substitution channel.¹³

Table 6 presents the second-stage results. The coefficients of the predicted O_3 are significantly negative in all columns, indicating that the policy-induced increase in ozone has caused significant deterioration in both bird abundance and bird species richness. These results provide evidence for Hypothesis 4: while the target-based regulation successfully achieved its goal of reducing $PM_{2.5}$, the unintended consequence of pollutant substitution directly caused a decline in biodiversity, constituting a major unforeseen ecological cost.

This finding is highly consistent with existing biological evidence. A large body of scientific research shows that high concentrations of O_3 can directly harm birds' respiratory

¹³This two-stage approach to analyzing mechanisms has been widely employed in the literature, for example, in [Lu \(2025\)](#) and [Li et al. \(2026\)](#).

Table 6: Mechanism Linking Pollutants to Bird Diversity Loss

	(1)	(2)
	Bird Abundance	Bird Species Richness
\widehat{O}_3	-0.727*** (0.243)	-0.299** (0.127)
Controls	Yes	Yes
City-Area FE	Yes	Yes
City-Year FE	Yes	Yes
Observations	1,194	1,194
R-squared	0.796	0.796

Notes: This table reports the second-stage results of the two-stage analytical framework. All columns include meteorological control variables, city-area fixed effects, and city-year fixed effects. Standard errors are clustered at the city-area level. * $p < 0.10$, ** $p < 0.05$, *** $p < 0.01$.

systems and indirectly destroy their habitats by damaging vegetation and reducing insect populations, their primary food sources (Agathokleous et al., 2020, 2023; Liang et al., 2020). Our econometric results confirm this scientific understanding in a real-world policy context.

5.3 Heterogeneous Effects across Ecological Guilds

To further deepen our understanding of these ecological costs, we explore whether the policy’s impact varies across different types of birds. We classify all bird species into six ecological guilds based on their primary diet and habitat: Piciformes (woodpeckers), Passeriformes (songbirds), Anseriformes (waterfowl), Gruiformes (waders), Galliformes (landfowl), and Falconiformes (raptors).¹⁴

Table 7 presents the heterogeneous results for bird abundance. Panel A shows that the policy had a significant negative impact on all guilds except for raptors. The magnitude of the effect is largest for waterfowl. Panel B, which reports the mechanism results, shows that the policy-induced O_3 increase has caused significant deterioration in abundance for woodpeckers, songbirds, waterfowl, waders and landfowls. Table 8 reports the results for bird species richness. The policy significantly reduced species richness for woodpeckers, songbirds and landfowl, with the largest negative impacts observed for smaller birds like woodpeckers and songbirds. The mechanism analysis in Panel B again confirms that the O_3

¹⁴This classification follows a common practice in biology.

Table 7: Heterogeneous Analysis for Bird Abundance by Ecological Guild

	(1)	(2)	(3)	(4)	(5)	(6)
	Bird Abundance					
	Woodpeckers	Songbirds	Waterfowl	Waders	Landfowl	Raptors
Panel A						
treat × post	-0.381*** (0.133)	-0.285** (0.116)	-0.615*** (0.207)	-0.338** (0.152)	-0.256* (0.144)	-0.320 (0.401)
Observations	794	1,144	606	748	768	350
R-squared	0.789	0.795	0.811	0.756	0.762	0.813
Panel B						
\widehat{O}_3	-0.555*** (0.194)	-0.415** (0.169)	-0.896*** (0.301)	-0.493** (0.222)	-0.373* (0.211)	-0.466 (0.584)
Observations	794	1,144	606	748	768	350
R-squared	0.789	0.795	0.811	0.756	0.762	0.813

Notes: This table reports heterogeneous effects on bird abundance across six ecological guilds. Panel A reports the baseline DID results. Panel B reports the second-stage results of the two-stage analytical framework. All regressions include control variables, city-area fixed effects, and city-year fixed effects. Standard errors are clustered at the city-area level. * $p < 0.10$, ** $p < 0.05$, *** $p < 0.01$.

increase is a key channel driving this loss of species richness.

These heterogeneous findings have a clear biological basis. First, raptors are apex predators, feeding on small mammals, whereas other guilds rely more heavily on insects and plants, which are known to be highly sensitive to O_3 damage (Hillstrom and Lindroth, 2008). Second, smaller birds like songbirds and woodpeckers have higher metabolic rates, leading to more frequent respiration and greater exposure to air pollutants, making them more physiologically vulnerable to direct O_3 damage (Liang et al., 2020). Our findings that the O_3 increase primarily harmed smaller, non-predatory birds are consistent with these biological priors and provide granular evidence on the structure of the policy’s ecological costs.

5.4 Supplementary Results: Alternative Measures of Biodiversity

In addition to the analysis focusing on bird diversity, we move beyond birds and demonstrate a more general impact of the policy on biodiversity. We use the Biodiversity Intactness Index (BII) created by the Natural History Museum, London as a more general measure of biodiversity (De Palma et al., 2024).¹⁵ The index reflects the abundance and diversity of

¹⁵Some limitations of the BII index prompted us to only use it as an alternative measure. First, unlike the data directly derived from observations of bird life activities, the BII is constructed by comparing terrestrial

Table 8: Heterogeneous Analysis for Bird Species Richness by Ecological Guild

	(1)	(2)	(3)	(4)	(5)	(6)
	Bird Species Richness					
	Woodpeckers	Songbirds	Waterfowl	Waders	Landfowl	Raptors
Panel A						
treat \times post	-0.198*** (0.059)	-0.122** (0.056)	-0.149 (0.097)	-0.089 (0.060)	-0.115** (0.056)	-0.199 (0.217)
Observations	794	1,144	606	748	768	350
R-squared	0.809	0.801	0.782	0.770	0.828	0.790
Panel B						
\widehat{O}_3	-0.289*** (0.086)	-0.178** (0.082)	-0.217 (0.141)	-0.130 (0.088)	-0.168** (0.081)	-0.290 (0.316)
Observations	794	1,144	606	748	768	350
R-squared	0.809	0.801	0.782	0.770	0.828	0.790

Notes: This table reports heterogeneous effects on bird species richness across six ecological guilds. Panel A reports the baseline DID results. Panel B reports the second-stage results of the two-stage analytical framework. All regressions include control variables, city-area fixed effects, and city-year fixed effects. Standard errors are clustered at the city-area level. * $p < 0.10$, ** $p < 0.05$, *** $p < 0.01$.

species in a given area. A higher BII value indicates a more intact ecosystem with greater species diversity and abundance, while a lower value suggests significant ecological disruption. We obtain the mean value of the index at the $0.1^\circ \times 0.1^\circ$ grid-year level and investigate the impact of the policy on overall biodiversity. Appendix G provides more details on our data description, sample construction, and identification strategy.

Panel A of Table A7 estimates the impact of the monitoring policy on general biodiversity measured by BII. The estimated coefficients of the interaction term are negative and statistically significant in all columns, indicating that the monitoring policy induced a significant deterioration in general biodiversity in treatment areas relative to control areas. Panel B further investigates the impact of policy-induced O_3 . The estimated coefficients of policy-induced O_3 concentrations are significantly negative in all columns, which indicates that the changes in O_3 concentrations induced by the monitoring policy are an important driving factor of biodiversity deterioration.

Overall, what we demonstrate in this subsection provides more general evidence of the monitoring policy's impact on biodiversity. The results shown in Table A7 are consistent

biodiversity across sites with varying human pressures, incorporating multiple confounding factors (e.g., habitat loss and human activity expansion), which may obscure the effect of air pollution. Second, unlike the bird data, which cover continuous annual observations, the BII is available only at five-year intervals, precluding annual analysis.

with our previous analysis of birds, revealing that the PM-targeted pollution control policy has led to a substitution between O₃ and PM_{2.5} concentrations, thereby inducing significant biodiversity deterioration.

6 Net Benefits: A Back-of-the-Envelope Calculation

In this section, having clearly demonstrated a logical chain from target-based regulations to pollutant substitutions to unexpected loss of biodiversity, we assess the net benefits associated with changes in PM_{2.5} and O₃ pollution induced by the policy. We conduct a back-of-the-envelope calculation that quantifies the health gains from PM_{2.5} reductions and the costs associated with higher ozone levels. The health gains here mainly consist of the reduction in deaths attributed to PM_{2.5} (Barwick et al., 2024), and the costs include the increase in deaths attributed to O₃ and the unintended loss of biodiversity.

6.1 Impact of the Policy on Pollutant Attributed Deaths

We begin this calculation by first estimating the effects of target-based environmental regulation on pollution-attributed deaths. We replace the dependent variable in Equation (1) with the grid-year level PM_{2.5}-attributed deaths (PAD_{PM_{2.5}}) and O₃-attributed deaths (PAD_{O₃}), and re-estimate the model using OLS. The construction of pollutant-attributed deaths are based on a well-established method developed by environmental and medical scientists (Abbasi-Kangevari et al., 2020; McDuffie et al., 2021; Malashock et al., 2022; Yang et al., 2025):

$$PAD_{it} = \sum_a \sum_d AgePop_{ia,2010} \times MB_{iad,2010} \times PAF_{iad,t} \quad (3)$$

$$AgePop_{iat} = POP_{i,2010} \times AgeP_{ia,2010}; \quad PAF_{iad,t} = \frac{RR_{ad} - 1}{RR_{ad}}$$

where i , t , a , and d denote the grid, year, age group, and disease, respectively. PAD_{it} represents the deaths attributable to pollution exposure at grid i in year t , determined by population factors ($AgePop$), baseline mortality factors (MB), and pollution factors (PAF). $AgePop_{ia,2010}$ is the population size of the age group a at grid i in the year 2010, decomposed into $POP_{i,2010}$ (total population) and $AgeP_{ia,2010}$ (proportion of the quinquennial age group).

$MB_{iad,2010}$ denotes the baseline mortality rate for disease d in age group a , grid i , and year 2010. Following the 2019 Global Burden of Disease Study (Abbasi-Kangevari et al., 2020), we focus on one disease strongly linked to O_3 exposure and six diseases strongly linked to $PM_{2.5}$ exposure.¹⁶ $PAF_{iad,t}$ represents the cause-specific population attributable fractions, which depend on the disease-specific relative risk of exposure (RR_{ad}), and RR_{ad} corresponds one-to-one with pollutant concentration. To control the effects of population, age proportion, and baseline mortality rate on pollutant attributed deaths, we keep $AgePop$ and MB at the 2010 levels, and only allow PAF to vary over time. Under this assumption, PAD_{it} in Equation (3) represents the pollutant-attributed deaths caused by changes in pollutant levels in grid i , year t .

Table 9 reports the results of the impact of target-based environmental regulation on pollutant-attributed deaths. In Panel A, we use the traditional fixed effect model. The dependent variables for Columns (1) to (3) are the $PM_{2.5}$ -attributed deaths and those for Columns (4) to (6) are O_3 -attributed deaths. The coefficients of the interaction term are both negative and statistically significant from Columns (1) to (3), indicating that the policy caused a significant decrease in $PM_{2.5}$ -attributed deaths in grids located in treatment areas, compared to grids in control areas. The coefficients of the interaction term are significantly positive from Columns (4) and (6), which suggests that the policy has led to a significant increase in O_3 -attributed deaths in treatment grids compared to control grids. Panel B replicates the analysis using the heterogeneity-robust difference-in-differences estimator proposed by Cengiz et al. (2019). The estimates maintain the same signs and statistical significance, as well comparable magnitudes, as those in Panel A.

Figure 6 demonstrates the dynamic effects on pollutant-attributed deaths. In addition to the traditional fixed effect model, we also use two heterogeneity-robust DID method from Cengiz et al. (2019) and Sun and Abraham (2021). Figure 6a shows that the estimated coefficients fluctuated around 0 prior to policy implementation. Following the introduction of the policy, the coefficients show a significant declining trend from about 0 to -20, with the downward trend becoming more apparent and significant. Figure 6b shows a completely different

¹⁶The disease strongly linked to O_3 exposure is chronic obstructive pulmonary disease (COPD), and diseases strongly linked to $PM_{2.5}$ exposure include COPD, lower respiratory infections, lung cancer, ischemic heart disease, stroke, and type 2 diabetes. For COPD, which is linked to both pollutants, the $PM_{2.5}$ and O_3 mortality burdens are computed separately using pollutant-specific concentration-response functions.

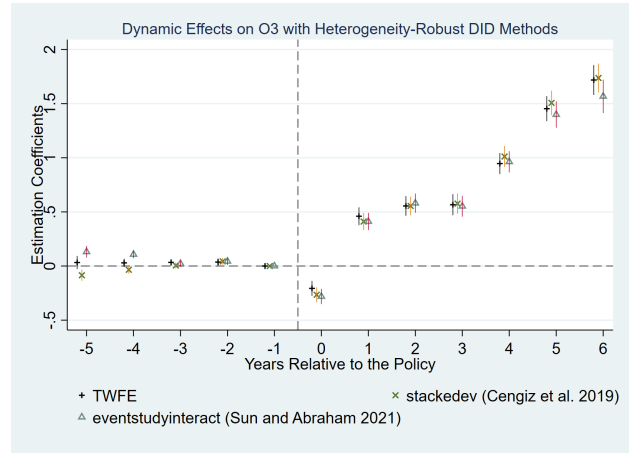
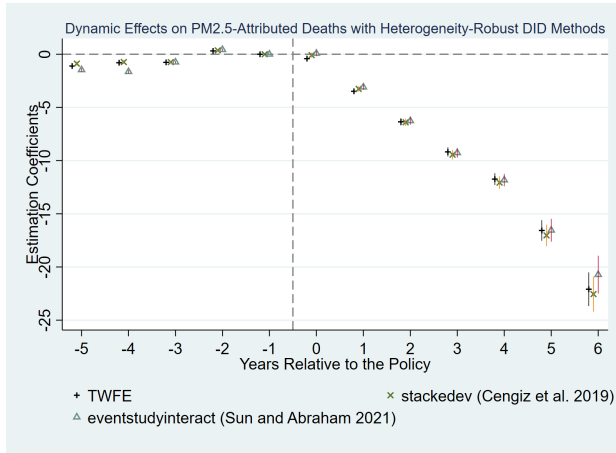
Table 9: Impact on Pollutant Attributed Deaths

	(1)	(2)	(3)	(4)	(5)	(6)
	PAD _{PM_{2.5}}			PAD _{O₃}		
Panel A: TWFE Model						
treat × post	-8.472*** (0.234)	-8.436*** (0.234)	-7.262*** (0.207)	1.584*** (0.058)	1.566*** (0.058)	1.282*** (0.047)
post	1.525*** (0.082)	1.478*** (0.081)		-0.403*** (0.023)	-0.383*** (0.023)	
Observations	904,830	904,830	904,830	904,830	904,830	904,830
R-squared	0.993	0.993	0.994	0.927	0.927	0.937
Panel B: Heterogeneity-Robust DID Method from Cengiz et al. (2019)						
ATT	-10.859*** (0.332)	-10.847*** (0.332)	-10.119*** (0.325)	2.090*** (0.084)	2.085*** (0.084)	1.900*** (0.081)
Controls	No	Yes	Yes	Yes	Yes	Yes
Grid FE	Yes	Yes	Yes	Yes	Yes	Yes
Province-Year FE	Yes	Yes	No	Yes	Yes	No
City-Year FE	No	No	Yes	No	No	Yes

Notes: This table reports the impact of target-based regulation on pollutant-attributed deaths. The dependent variables in Columns (1) to (3) are the grid-year level PM_{2.5}-attributed death and those in Columns (4) to (6) are O₃-attributed deaths. Panel A uses TWFE models with interactive fixed effects and Panel B uses a heterogeneity-robust DID method from [Cengiz et al. \(2019\)](#) to alleviate the heterogeneous treatment problems. All columns control for grid fixed effects. Meteorological control variables are controlled in Columns (2) (3), (5), and (6). Columns (1), (2), (4), and (5) control the province-year fixed effects while Columns (3) and (6) control the city-year fixed effects. Standard errors are clustered at the grid level. * $p < 0.10$, ** $p < 0.05$, *** $p < 0.01$.

trend. The coefficients before the implementation still fluctuate around 0. However, the coefficients after the implementation rise significantly from about 0 to 1.7, indicating that the relative increase in O₃-attributed deaths in treatment areas after the policy implementation is a long-term and stable trend.

We also conduct placebo tests for the results in Table 9, using the same methods as those in Section 4.3. The results are plotted in Figure [A2e](#) and [A2f](#). The red lines, indicating the baseline estimated coefficients, lie outside the 99% confidence intervals of the placebo estimator distributions, which verifies the robustness of the results shown in Table 9.



(a) Dynamic Effects on PM_{2.5}-Attributed Deaths

(b) Dynamic Effects on O₃-Attributed Deaths

Figure 6: Dynamic Effects on Pollutant-Attributed Deaths

Notes: This figure plots the dynamic effects on the pollutant-attributed deaths with different models. The dots represent point-estimated coefficients and the shaded areas represent 90% confidence intervals. All models include meteorological control variables, grid fixed effects, and city-year fixed effects. Standard errors are clustered at the grid level. The year prior to the policy ($k = -1$) is the omitted base category.

6.2 Benefits and Costs from Pollutant-Attributed Deaths

The health gains of the policy mainly come from the reduction of PM_{2.5}-attributed deaths. The mortality benefit is quantified using the age-adjusted value of statistical life (VSL). The VSL approach is commonly used by policymakers and researchers to evaluate the benefits of life-saving regulations. Due to the lack of reliable VSL estimates for the Chinese population, we use a benefit transfer method that infers the VSL for Chinese residents from US-based VSL estimates and the income elasticity of VSL. This benefit-transfer method is commonly used for countries with insufficient or unreliable VSL data (Viscusi and Masterman, 2017).

We use \$1.54 million (1997 dollars), the VSL in the United States from Ashenfelter and Greenstone (2004), as the baseline value, which is widely used in economic research (Watson, 2006; Bailey and Goodman-Bacon, 2015; Barwick et al., 2024). Narain and Sall (2016) suggest a transfer elasticity of 1.2 for transferring the VSL from the United States to developing countries. Following Barwick et al. (2024), we also consider a one-to-nine income ratio between China and United States. Combined with the CPI, the VSL in China is about \$0.21 million (2015 dollars).¹⁷

As shown in Table 9, Column (3), the regulation policy led to an average decrease of

¹⁷First, we transform \$1.54 million (1997 dollars) into \$2.3 million (2015 dollars) based on the CPI. Second, we calculate the VSL in China = $\$2.3 / (1.2 \times 9) = \0.21 million (2015 dollars).

7.262 PM_{2.5}-attributed deaths in the treatment grids compared to the control grids. There are 43,400 urban grids in our research sample, which suggests that the policy reduced the number of deaths in treatment areas by about 315,170.8. Therefore, the benefit from the reduction of PM_{2.5}-attributed deaths is about \$66,185.868 million (2015 dollars).

However, the policy also induced unintended health costs because of the increases in O₃ concentrations. Similar to the calculation of gains from the reduction of PM_{2.5}-attributed deaths, the cost of the increase in O₃-attributed deaths is approximately \$11,684.148 million (2015 dollars).¹⁸

6.3 Costs from Biodiversity Loss

Another unintended cost of the increases in O₃ concentrations is incurred due to the loss of biodiversity. Specifically, the results of Column (3) in Table 5 show that the policy led to a 0.340 decline in bird abundance in the treatment areas compared to the control areas. Combined with Equation (E.1), the result in Table 5, Column (3) indicates that the number of observed birds in treatment areas decreased by about 28.8% compared to control areas.¹⁹

The mean value of willingness to pay (WTP) for protecting bird diversity is approximately \$75.79 (2020 dollars) per household per year (Lundhede et al., 2014; Martín-López et al., 2008; Sharma and Kreye, 2022; Meng et al., 2025). Applying this to China's 202,764,700 urban households (2020 Census),²⁰ the ecological costs of the target-based environmental regulation are \$4,053.194 million (2015 dollars) when measured by bird abundance.²¹

The above calculation indicates that if we take the O₃-attributed deaths caused by the pollution substitution into account, the health gains from the decreases in PM_{2.5} concentrations will be offset by about 17.7%. If bird diversity is further taken into account, the benefits will be additionally offset by about 6.1%.²² It should be particularly noted that bird diversity

¹⁸ $43400 \times 1.282 \times \$0.21\text{million (2015 dollars)} = \$11,684.148\text{ million (2015 dollars)}$

¹⁹According to Equation (E.1), a 0.340 reduction of Γ_{ict} led to a $e^{-0.340} - 1 \approx -0.288$ decline in the number of observed birds. Analogously, a 0.140 reduction of Γ_{ict} led to a $e^{-0.140} - 1 \approx -0.131$ decline in the number of observed bird species.

²⁰The data is from the 2020 China Population Census Yearbook.

²¹The cost of bird abundance loss = $(28.8\% \times \$75.79 \times 202,764,700) / 1000000 = \$4,425.851\text{ million (2020 dollars)} = \$4,425.851\text{ million} \times 0.9158 = \$4,053.194\text{ million (2015 dollars)}$. If measured by bird species richness, the costs will be $\$1,843.640\text{ (2015 dollars)}$. $(13.1\% \times \$75.79 \times 202,764,700) / 1000000 = \$2,013.147\text{ million (2020 dollars)} = \$2,013.147\text{ million} \times 0.9158 = \$1,843.640\text{ million (2015 dollars)}$.

²² $11,684.148 / 66,185.868 \approx 17.7\%$; $4,053.194 / 66,185.868 \approx 6.1\%$

Table 10: Calculation Results of the Net Benefits

	Benefit for health induced by PM _{2.5} decline	Cost for health induced by O ₃ increase	Cost for bird diversity loss (measured by bird abundance)
Change	315,170.8	55,638.8	28.8%
Value	\$0.21 million (2015 dollars per person)		\$75.79 (2020 dollars per household per year)
Total Value (million 2015 dollars)	\$66,185.868	\$11,684.148	\$4,053.194
Ratio (Relative to Benefits)	100%	17.7%	6.1%

Notes: This table compares the health benefits from PM_{2.5} reduction with the health and ecological costs from O₃ increase. Total values are all converted to 2015 dollars.

is only a small part of the ecosystem, so the ecological costs estimated in this paper are far from the whole and should be considered as a lower bound. In conclusion, if the increases in O₃ concentrations caused by the target-based policy are incorporated into the calculation framework, the PM_{2.5} benefits are offset by at least 23.8%. A summary of the calculation results is presented in Table 10.

7 Conclusion and Implications

Air pollution control remains a worldwide challenge. This is reflected not only in the pollutant leakage between regulated and unregulated regions, but also in pollutant substitution, another “leakage” across pollutants, rooted in the multitask principal–agent problem, which is documented in our paper. While the former has received extensive attention in the literature, the latter is relatively neglected.

We provide robust evidence of the pollution substitution phenomenon and its unintended costs induced by China’s PM-targeted War on Pollution. Our study finds that the PM_{2.5} concentration in treated urban areas significantly declined relative to control rural areas, while the O₃ concentration significantly increased. We argue that this phenomenon is driven by a political economy mechanism rooted in the structure of environmental accountability. In order to achieve the assessment standard, local governments prioritized abatement of the most salient and easily controlled sources of particulate pollution—even

if doing so meant neglecting other pollutants. Crucially, the increased O₃ pollution significantly harms human health and even biodiversity, which are unintended but long-term threatening consequences. We conduct a back-of-the-envelope calculation of the net benefits associated with changes in PM_{2.5} and O₃ pollution induced by the policy. The results show that the benefits of the policy will be offset by approximately 23-24 percent if the health and ecological costs of O₃ are taken into account. Moreover, since bird diversity is only one proxy for ecosystem health, this represents a conservative estimate of the true ecological costs.

Our analyses provide several policy implications for pollution abatement. First, effective governance should institutionalize multi-pollutant accountability. The pollutant substitution identified in our paper stems from the incomplete assessment standards in China's first stage of air pollution abatement. A comprehensive assessment framework for air pollution abatement must cover all major pollutants. Although China's new *Action Plan for Continuous Improvement of Air Quality*, issued in late 2023, explicitly elevates the co-control of PM_{2.5} and O₃ and the co-abatement of NO_x and VOCs to the level of national strategy, many other jurisdictions likely face this multi-pollutant problem and have yet fixed their policies. Second, researchers should integrate ecosystem health indicators into evaluation frameworks. The biodiversity decline we document reveals that meeting pollutant concentration targets does not ensure ecological recovery. A coordinated and sustainable environmental governance system should progressively incorporate comprehensive ecological health metrics, including biodiversity indicators and ecosystem service functions, into performance evaluations. This transition from pollution control to ecosystem health represents the fundamental criterion for sustainable development.

Our study is, of course, not without limitations. Bird diversity is but one proxy for ecosystem health; future research could explore impacts on water quality, soil health, and agricultural productivity. Our findings illustrate how governance systems optimized for one metric can generate real but incomplete progress. Effective multi-pollutant policy requires accountability frameworks that are as ecologically integrated as the systems they seek to govern.

References

- Abbasi-Kangevari, M., Abd-Allah, F., Adekanmbi, et al. (2020). Global burden of 87 risk factors in 204 countries and territories, 1990–2019: a systematic analysis for the global burden of disease study 2019. *The Lancet (British edition)*, 396(10258):1223–1249.
- Acharya, V. V., Schnabl, P., and Suarez, G. (2013). Securitization without risk transfer. *Journal of Financial Economics*, 107(3):515–536.
- Agathokleous, E., Feng, Z., Oksanen, E., et al. (2020). Ozone affects plant, insect, and soil microbial communities: A threat to terrestrial ecosystems and biodiversity. *Science Advances*, 6(33):eabc1176.
- Agathokleous, E., Sicard, P., Feng, Z., and Paoletti, E. (2023). Ozone pollution threatens bird populations to collapse: An imminent ecological threat? *Journal of Forestry Research*, 34(6):1653–1656.
- Ambec, S. and Coria, J. (2013). Prices vs quantities with multiple pollutants. *Journal of Environmental Economics and Management*, 66(1):123–140.
- Ashenfelter, O. and Greenstone, M. (2004). Using mandated speed limits to measure the value of a statistical life. *The Journal of Political Economy*, 112(S1):S226–S267.
- Bailey, M. J. and Goodman-Bacon, A. (2015). The war on poverty’s experiment in public medicine: Community health centers and the mortality of older Americans. *The American Economic Review*, 105(3):1067–1104.
- Balboni, C. and Shapiro, J. S. (2025). Spatial environmental economics. In *Handbook of Regional and Urban Economics*, volume 6, pages 585–652. Elsevier.
- Barwick, P. J., Li, S., Lin, L., and Zou, E. Y. (2024). From fog to smog: The value of pollution information. *American Economic Review*, 114(5):1338–1381.
- Bertrand, M. and Mullainathan, S. (2001). Are ceos rewarded for luck? the ones without principals are*. *The Quarterly Journal of Economics*, 116(3):901–932.
- Bi, X. (2017). Cleansing the air at the expense of waterways? Empirical evidence from the toxic releases of coal-fired power plants in the United States. *Journal of Regulatory Economics*, 51(1):18–40.
- Borusyak, K., Jaravel, X., and Spiess, J. (2024). Revisiting event-study designs: Robust and efficient estimation. *Review of Economic Studies*, 91(6):3253–3285.

- Brei, M., Pérez-Barahona, A., and Strobl, E. (2016). Environmental pollution and biodiversity: Light pollution and sea turtles in the caribbean. *Journal of Environmental Economics and Management*, 77:95–116.
- Cengiz, D., Dube, A., Lindner, A., and Zipperer, B. (2019). The effect of minimum wages on low-wage jobs. *The Quarterly Journal of Economics*, 134(3):1405–1454.
- Chen, Y., Li, P., and Lu, Y. (2018). Career concerns and multitasking local bureaucrats: Evidence of a target-based performance evaluation system in China. *Journal of Development Economics*, 133:84–101.
- Cohen, A. J., Brauer, M., Burnett, R., et al. (2017). Estimates and 25-year trends of the global burden of disease attributable to ambient air pollution: An analysis of data from the Global Burden of Diseases Study 2015. *The Lancet*, 389(10082):1907–1918.
- Dallmann, T. R., DeMartini, S. J., Kirchstetter, T. W., et al. (2012). On-road measurement of gas and particle phase pollutant emission factors for individual heavy-duty diesel trucks. *Environmental science & technology*, 46(15):8511–8518.
- De Palma, A., Contu, S., et al. (2024). The biodiversity intactness index developed by the natural history museum, london, v2.1.1 (open access, limited release).
- Dranove, D., Kessler, D., McClellan, M., and Satterthwaite, M. (2003). Is more information better? The effects of “report cards” on health care providers. *The Journal of Political Economy*, 111(3):555–588.
- Duflo, E., Greenstone, M., Pande, R., and Ryan, N. (2018). The value of regulatory discretion: Estimates from environmental inspections in India. *Econometrica*, 86(6):2123–2160.
- Ebenstein, A., Fan, M., Greenstone, M., He, G., and Zhou, M. (2017). New evidence on the impact of sustained exposure to air pollution on life expectancy from China’s Huai River Policy. *Proceedings of the National Academy of Sciences*, 114(39):10384–10389.
- Feng, J., Huang, W., Smyth, R., and Yao, Y. (2025). Automatic air quality monitoring and “unintended” water pollution: Evidence from China. *Available at SSRN 5375361*.
- Figlio, D. N. and Winicki, J. (2005). Food for thought: The effects of school accountability plans on school nutrition. *Journal of Public Economics*, 89(2):381–394.
- Frank, E. and Sudarshan, A. (2024). The social costs of keystone species collapse: Evidence from the decline of vultures in India. *American Economic Review*, 114(10):3007–3040.

- Frank, E. G. (2024). The economic impacts of ecosystem disruptions: Costs from substituting biological pest control. *Science*, 385(6713):eadg0344.
- Fullerton, D. and Karney, D. H. (2018). Multiple pollutants, co-benefits, and suboptimal environmental policies. *Journal of Environmental Economics and Management*, 87:52–71.
- Geruso, M. and Layton, T. (2020). Upcoding: Evidence from medicare on squishy risk adjustment. *The Journal of Political Economy*, 128(3):984–1026.
- Ghanem, D. and Zhang, J. (2014). “Effortless perfection”: Do chinese cities manipulate air pollution data? *Journal of Environmental Economics and Management*, 68(2):203–225.
- Gibson, M. (2019). Regulation-induced pollution substitution. *The Review of Economics and Statistics*, 101(5):827–840.
- Goodman-Bacon, A. (2021). Difference-in-differences with variation in treatment timing. *Journal of Econometrics*, 225(2):254–277.
- Greenstone, M., He, G., Jia, R., and Liu, T. (2022). Can technology solve the principal-agent problem? evidence from China’s war on air pollution. *American Economic Review: Insights*, 4(1):54–70.
- He, G., Wang, S., and Zhang, B. (2020). Watering down environmental regulation in China. *The Quarterly Journal of Economics*, 135(4):2135–2185.
- Heckman, J. J., Heinrich, C., and Smith, J. A. (2002). The performance of performance standards. *Journal of Human Resources*, 37(4):778–811.
- Hillstrom, M. L. and Lindroth, R. L. (2008). Elevated atmospheric carbon dioxide and ozone alter forest insect abundance and community composition. *Insect Conservation and Diversity*, 1(4):233–241.
- Holmström, B. and Milgrom, P. (1991). Multitask principal-agent analyses: Incentive contracts, asset ownership, and job design. *Journal of Law, Economics, & Organization*, 7(Special Issue):24–52.
- Hong, H. and Chen, K. (2026). When the fire ends: Straw burning, regulation, and pollution substitution. *Journal of Development Economics*, 181:103727.
- Jacob, B. A. and Levitt, S. D. (2003). Rotten apples: An investigation of the prevalence and predictors of teacher cheating. *The Quarterly Journal of Economics*, 118(3):843–877.
- Le, T., Wang, Y., Liu, L., et al. (2020). Unexpected air pollution with marked emission reduc-

- tions during the covid-19 outbreak in China. *Science*, 369(6504):702–706.
- Li, C., Chen, J., Liao, X., et al. (2023). Shorebirds-driven trophic cascade helps restore coastal wetland multifunctionality. *Nature Communications*, 14(1):8076–14.
- Li, K., Jacob, D. J., Liao, H., et al. (2021). Ozone pollution in the North China Plain spreading into the late-winter haze season. *Proceedings of the National Academy of Sciences*, 118(10):e2015797118.
- Li, K., Jacob, D. J., Liao, H., Shen, L., Zhang, Q., and Bates, K. H. (2019). Anthropogenic drivers of 2013–2017 trends in summer surface ozone in China. *Proceedings of the National Academy of Sciences*, 116(2):422–427.
- Li, M., Liu, H., Geng, G., et al. (2017). Anthropogenic emission inventories in China: a review. *National Science Review*, 4(6):834–866.
- Li, X., Liu, Z., Peng, Y., and Xu, Z. (2026). Bank risk-taking, credit allocation, and monetary policy transmission: Evidence from china. *American Economic Journal: Macroeconomics*, 18(1):384–415.
- Liang, Y., Rudik, I., Zou, E. Y., Johnston, A., Rodewald, A. D., and Kling, C. L. (2020). Conservation cobenefits from air pollution regulation: Evidence from birds. *Proceedings of the National Academy of Sciences*, 117(49):30900–30906.
- Lu, S. (2025). Green bonds: reputational bonding via media coverage. *Management Science*.
- Lundhede, T. H., Jacobsen, et al. (2014). Public support for conserving bird species runs counter to climate change impacts on their distributions. *PloS one*, 9(7):e101281.
- Malashock, D. A., Delang, M. N., Becker, J. S., et al. (2022). Global trends in ozone concentration and attributable mortality for urban, peri-urban, and rural areas between 2000 and 2019: a modelling study. *The Lancet Planetary Health*, 6(12):e958–e967.
- Marder, E., Smiley, T. M., Yanites, B. J., and Kravitz, K. (2025). Direct effects of mountain uplift and topography on biodiversity. *Science*, 387(6740):1287–1291.
- Martín-López, B., Montes, C., and Benayas, J. (2008). Economic valuation of biodiversity conservation: the meaning of numbers. *Conservation biology*, 22(3):624–635.
- Matthews, T. J., Triantis, K. A., Wayman, J. P., et al. (2024). The global loss of avian functional and phylogenetic diversity from anthropogenic extinctions. *Science (American Association for the Advancement of Science)*, 386(6717):55–60.

- McDuffie, E. E., Martin, R. V., et al. (2021). Source sector and fuel contributions to ambient PM_{2.5} and attributable mortality across multiple spatial scales. *Nature communications*, 12(1):3594–12.
- Meng, L., Liu, P., Zhou, Y., and Mei, Y. (2025). Blaming the wind? The impact of wind turbine on bird biodiversity. *Journal of Development Economics*, 172:103402.
- Narain, U. and Sall, C. (2016). Methodology for valuing the health impacts of air pollution: Discussion of challenges and proposed solutions. Technical report, World Bank, Washington, DC.
- Neal, D. and Whitmore Schanzenbach, D. (2010). Left behind by design: Proficiency counts and test-based accountability. *The Review of Economics and Statistics*, 92(2):263–283.
- Purvis, A. and Hector, A. (2000). Getting the measure of biodiversity. *Nature*, 405(6783):212–219.
- Qian, H., Xu, S., Cao, J., Ren, F., Wei, W., Meng, J., and Wu, L. (2021). Air pollution reduction and climate co-benefits in China’s industries. *Nature Sustainability*, 4(5):417–425.
- Qin, R. and Zhang, F. (2022). HRLT: A high-resolution (1 day, 1 km) and long-term (1961–2019) gridded dataset for temperature and precipitation across China.
- Richard, F. J., Gigauri, M., Bellini, G., Rojas, O., and Runde, A. (2021). Warning on nine pollutants and their effects on avian communities. *Global Ecology and Conservation*, 32:e01898.
- Shao, M., Zhang, Y., Zeng, L., et al. (2009). Ground-level ozone in the pearl river delta and the roles of voc and nox in its production. *Journal of Environmental Management*, 90(1):512–518.
- Sharma, S. and Kreye, M. M. (2022). Social value of bird conservation on private forest lands in pennsylvania, usa. *Ecological economics*, 196:107426.
- Shimshack, J. P. (2014). The economics of environmental monitoring and enforcement. *Annual Review of Resource Economics*, 6:339–360.
- Smith, S. J., van Aardenne, J., Klimont, Z., et al. (2011). Anthropogenic sulfur dioxide emissions: 1850–2005. *Atmospheric Chemistry and Physics*, 11(3):1101–1116.
- Southerland, V. A., Brauer, M., Mohegh, A., et al. (2022). Global urban temporal trends in fine particulate matter (PM_{2.5}) and attributable health burdens: Estimates from global datasets. *The Lancet Planetary Health*, 6(2):e139–e146.

- Sun, L. and Abraham, S. (2021). Estimating dynamic treatment effects in event studies with heterogeneous treatment effects. *Journal of econometrics*, 225(2):175–199.
- Taylor, M. S. and Mayer, F. (2023). International trade, noise pollution, and killer whales. NBER Working Paper 31390, National Bureau of Economic Research.
- Uchida, K., Matanle, P., Li, Y., Fujita, T., and Hiraiwa, M. K. (2025). Biodiversity change under human depopulation in Japan. *Nature Sustainability*, pages 1–11. Advance online publication.
- Viscusi, W. K. and Masterman, C. J. (2017). Income elasticities and global values of a statistical life. *Journal of Benefit-Cost Analysis*, 8(2):226–250.
- Wang, N., Lyu, X., Deng, X., et al. (2019). Aggravating O₃ pollution due to nox emission control in eastern China. *Science of the Total Environment*, 677:732–744.
- Wang, Y., Yang, Y., Yuan, Q., et al. (2025). Substantially underestimated global health risks of current ozone pollution. *Nature Communications*, 16(1):102–15.
- Watson, T. (2006). Public health investments and the infant mortality gap: Evidence from federal sanitation interventions on u.s. indian reservations. *Journal of Public Economics*, 90(8):1537–1560.
- Wei, J., Li, Z., Li, K., et al. (2022). Full-coverage mapping and spatiotemporal variations of ground-level ozone (O₃) pollution from 2013 to 2020 across China. *Remote Sensing of Environment*, 270:112775.
- Wei, J., Li, Z., Lyapustin, A., et al. (2021). Reconstructing 1-km-resolution high-quality pm_{2.5} data records from 2000 to 2018 in China: spatiotemporal variations and policy implications. *Remote Sensing of Environment*, 252:112136.
- Wei, J., Li, Z., Lyapustin, A., et al. (2023). First close insight into global daily gapless 1 km pm_{2.5} pollution, variability, and health impact. *Nature communications*, 14(1):8349.
- Yang, L., Lin, Y., Wang, J., and Peng, F. (2024). Achieving air pollution control targets with technology-aided monitoring: Better enforcement or localized efforts? *American Economic Journal: Economic Policy*, 16(4):280–315.
- Yang, Z., Li, Z., Cheng, F., et al. (2025). Two-decade surface ozone pollution in China: Enhanced fine-scale estimations and environmental health implications. *Remote Sensing of Environment*, 317:114459.

- Zhao, M., Cheng, C., Zhou, Y., et al. (2021). A global dataset of annual urban extents (1992–2020) from harmonized nighttime lights. *Earth System Science Data Discussions*, pages 1–25. Preprint.
- Zheng, B., Cheng, J., Geng, G., et al. (2021). Mapping anthropogenic emissions in China at 1 km spatial resolution and its application in air quality modeling. *Science Bulletin*, 66(6):612–620.
- Zheng, B., Tong, D., Li, M., et al. (2018). Trends in China’s anthropogenic emissions since 2010 as the consequence of clean air actions. *Atmospheric chemistry and physics*, 18(19):14095–14111.
- Zou, E. Y. (2021). Unwatched pollution: The effect of intermittent monitoring on air quality. *American Economic Review*, 111(7):2101–2126.

Appendix

A Appendix Tables and Figures

Table A1: Descriptive Statistics of Main Variables

	Observations	Mean	Standard Deviation	Min	Max
Panel A: $0.1^\circ \times 0.1^\circ$ grid-year level					
PM _{2.5}	904,743	42.05	17.56	7.90	153.93
O ₃	904,743	84.42	12.66	36.76	129.89
<i>treat</i>	904,743	0.05	0.21	0	1
<i>post</i>	904,743	0.54	0.50	0	1
PAD_PM _{2.5}	904,830	13.14	43.63	0	3,223.71
PAD_O ₃	904,830	1.21	3.63	0	334.28
BII	445,645	45.29	18.08	1.92	89.95
Panel B: $0.25^\circ \times 0.25^\circ$ grid-year level					
ln PM _{2.5}	148,720	3.87	2.66	0	11.15
ln SO ₂	148,720	3.69	2.95	0	12.97
ln NO _x	148,720	4.32	2.93	0	11.94
ln VOCs	148,720	4.65	2.84	0	12.48
Panel C: city–area–year level					
Bird Abundance	2,330	-0.87	1.13	-5.87	2.66
Bird Species Richness	2,330	-0.25	0.61	-3.17	1.78
<i>post</i>	2,330	0.66	0.47	0	1
<i>treat</i>	2,330	0.31	0.46	0	1
mean maximum temperature (K)	7,230	292.43	5.29	275.98	303.89
mean minimum temperature (K)	7,230	282.72	7.09	262.37	295.99
mean precipitation (m)	7,230	2.67	1.48	0.17	9.05

Notes: This table presents descriptive statistics for key variables. Panel A shows variables at the $0.1^\circ \times 0.1^\circ$ grid-year level; Panel B shows variables at the $0.25^\circ \times 0.25^\circ$ grid-year level; Panel C shows variables at the city–area–year level.

Table A2: Robustness Checks: Alternative Definitions of Urban Areas and Other Sample Selections

Year Sample	(1)	(2)	(3)	(4)	(5)	(6)
	2010–2019				2000–2019	
	PM _{2.5}	O ₃	PM _{2.5}	O ₃	PM _{2.5}	O ₃
treat × post	−0.961*** (0.047)	0.748*** (0.053)	−0.654*** (0.027)	0.467*** (0.030)	−0.380*** (0.031)	0.505*** (0.032)
Controls	Yes	Yes	Yes	Yes	No	No
Grid FE	Yes	Yes	Yes	Yes	Yes	Yes
City–Year FE	Yes	Yes	Yes	Yes	Yes	Yes
Observations	904,830	904,743	612,470	612,384	1,809,660	1,809,256
R-squared	0.988	0.962	0.993	0.978	0.989	0.974

Notes: The table reports robustness checks for the baseline regression. Dependent variables are the annual average PM_{2.5} concentration (odd-numbered columns) and O₃ concentration (even-numbered columns) at the grid level. Columns (1)–(2) use a stricter definition of “urban area”, including only built-up areas within the municipal districts. Columns (3)–(4) exclude samples from the Tibet and Xinjiang autonomous regions. Columns (5)–(6) extend the sample period to 2000–2019. All regressions include grid fixed effects and city-year fixed effects. Robust standard errors, clustered at the grid level, are in parentheses. * $p < 0.10$, ** $p < 0.05$, *** $p < 0.01$.

Table A3: Impact of Target-based Environmental Regulations on Pollutant Concentrations: Regressions at the City–Area–Year Level

	(1)	(2)	(3)	(4)	(5)	(6)
	PM _{2.5}			O ₃		
	treat × post	−1.351*** (0.238)	−1.325*** (0.235)	−1.221*** (0.103)	0.489** (0.235)	0.398* (0.233)
post	0.662** (0.331)	0.585* (0.330)		−2.287*** (0.390)	−2.220*** (0.382)	
Controls	No	Yes	Yes	No	Yes	Yes
City–Area FE	Yes	Yes	Yes	Yes	Yes	Yes
Province–Year FE	Yes	Yes	No	Yes	Yes	No
City–Year FE	No	No	Yes	No	No	Yes
Observations	6,570	6,570	6,520	6,570	6,570	6,520
R-squared	0.981	0.981	0.997	0.933	0.936	0.986

Notes: This table reports regression results based on panel data at the city-area-year level. Meteorological control variables are controlled in Columns (2), (3), (5), and (6). Columns (1) (2), (4), and (5) control the province-year fixed effects, and Columns (3) and (6) control the city-year fixed effects. Standard errors are clustered at the city-area level. * $p < 0.10$, ** $p < 0.05$, *** $p < 0.01$.

Table A4: Robustness Checks: Alternative Model Specifications and Controlling for Concurrent Policy Interference

	(1)	(2)	(3)	(4)
	PM _{2.5}	O ₃	PM _{2.5}	O ₃
treat × post	-0.847*** (0.0525)	1.493*** (0.0567)	-0.576*** (0.0299)	0.594*** (0.0337)
post	0.461*** (0.0271)	-2.115*** (0.0319)		
Observations	876,530	876,443	890,459	890,375
R-squared	0.979	0.936	0.988	0.963
Controls	Yes	Yes	Yes	Yes
Province-Year FE	Yes	Yes	No	No
Grid FE	Yes	Yes	Yes	Yes
City-Specific Time Trends	Yes	Yes	Yes	Yes
City-Year FE	No	No	Yes	Yes
Key Ecological Zones	No	No	Yes	Yes

Notes: This table reports further robustness checks. The dependent variable is the annual average concentration of PM_{2.5}, O₃, or PM₁₀ at the grid-year level, as indicated by the column headers. Columns (1)–(2) control for flexible city-level time trends by including interactions between the baseline (2010) city level ln population, ln GDP per capita, PM_{2.5} concentration and administrative area. Columns (3)–(4) control for potential interference from the concurrent *National Key Ecological Functional Zones* policy. Considering that the designations were announced in the second half of the year and effects may lag, we use 2011 and 2017 as policy shock years, treating counties designated as key ecological functional zones as the treatment group and the rest as control. Robust standard errors clustered at the grid level are in parentheses. * $p < 0.10$, ** $p < 0.05$, *** $p < 0.01$.

Table A5: Robustness Checks: Alternative Clustering Level

	(1)	(2)	(3)	(4)	(5)	(6)
	PM _{2.5}			O ₃		
treat × post	-1.391*** (0.156)	-1.416*** (0.151)	-0.573*** (0.081)	0.938*** (0.127)	0.918*** (0.122)	0.560*** (0.074)
post	0.908*** (0.342)	0.933*** (0.335)		-0.630 (0.486)	-0.668 (0.503)	
Controls	No	Yes	Yes	No	Yes	Yes
Province-Year FE	Yes	Yes	No	Yes	Yes	No
Grid FE	Yes	Yes	Yes	Yes	Yes	Yes
City-Year FE	No	No	Yes	No	No	Yes
Observations	904,743	904,743	904,743	904,743	904,743	904,743
R-squared	0.976	0.976	0.988	0.927	0.928	0.962
Cluster	City	City	City	City	City	City

Notes: This table replicates the baseline results in Table 1 Panel A with standard errors clustered at the prefecture-city level. All columns control grid fixed effects. Meteorological control variables are controlled in columns (2) (3) (5) and (6). Columns (1) (2) (4) (5) control the province-year fixed effects and columns (3) and (6) control the city-year fixed effects. * $p < 0.10$, ** $p < 0.05$, *** $p < 0.01$.

Table A6: Separation of Pathways for O₃ Deterioration

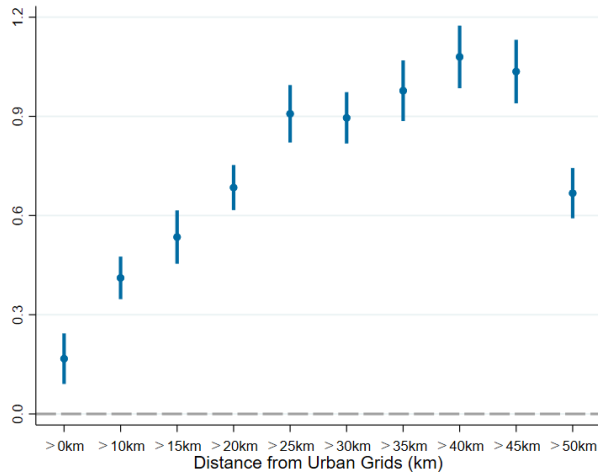
	(1)	(2)
	PM _{2.5}	O ₃
$\widehat{PM}_{2.5}$		-0.721** (0.285)
SO ₂	0.255*** (0.045)	
NO _x	0.068 (0.119)	-0.358*** (0.134)
VOCs	-0.428*** (0.123)	0.326** (0.146)
NO _x ²	-0.039** (0.015)	0.022* (0.013)
VOCs ²	0.012 (0.009)	-0.010 (0.011)
NO _x × VOCs	0.017 (0.018)	-0.001 (0.025)
Controls	Yes	Yes
City-Year FE	Yes	Yes
Grid FE	Yes	Yes
Observations	148,440	148,408
R-squared	0.965	0.964

Notes: This table reports the results of the separation of two pathways for O₃ Deterioration. All columns include meteorological control variables, grid fixed effects, and city-year fixed effects. Standard errors are clustered at the grid level. * $p < 0.10$, ** $p < 0.05$, *** $p < 0.01$.

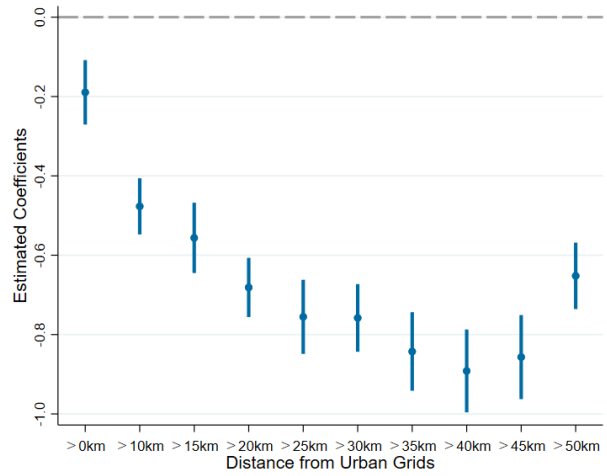
Table A7: The Impact of Monitoring Policy on General Biodiversity

	(1)	(2)	(3)
	BII		
<hr/>			
Panel A			
treat × post	-0.912*** (0.022)	-0.904*** (0.022)	-0.770*** (0.022)
Controls	No	Yes	Yes
Grid FE	Yes	Yes	Yes
Province-Year FE	Yes	Yes	No
City-Year FE	No	No	Yes
Observations	445,645	445,645	445,645
R-squared	0.995	0.995	0.996
<hr/>			
Panel B			
\widehat{O}_3	-0.878*** (0.021)	-0.873*** (0.021)	-1.060*** (0.030)
Controls	No	Yes	Yes
Grid FE	Yes	Yes	Yes
Province-Year FE	Yes	Yes	No
City-Year FE	No	No	Yes
Observations	445,638	445,638	445,638
R-squared	0.995	0.995	0.996

Notes: This table reports the impact of monitoring policy on general biodiversity. The dependent variables are the annual average value Biodiversity Intactness Index at the grid level, and a higher value indicates a more intact ecosystem with greater species diversity and abundance. Panel A shows the results of the overall impact of monitoring policy on general biodiversity. Panel B further shows the impact of policy-induced O_3 on biodiversity, which only includes the 2nd stage results. Due to the time discontinuity of BII data, the sample years in the table are 2000, 2005, 2010, 2015, and 2020. Since the meteorological data from [Qin and Zhang \(2022\)](#) only cover up to 2019, we use the average meteorological values of other years as the observed meteorological values for 2020. * $p < 0.10$, ** $p < 0.05$, *** $p < 0.01$.



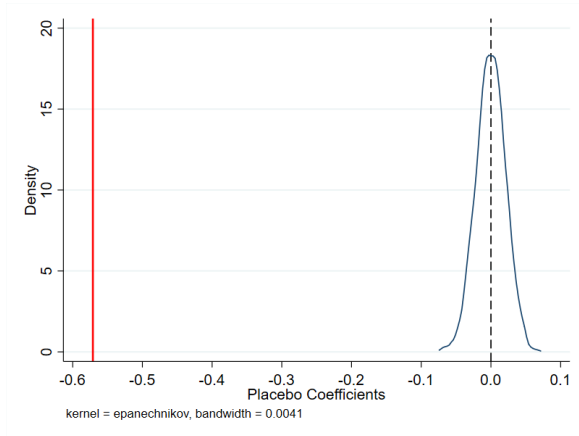
(a) Effects on PM_{2.5} Concentrations



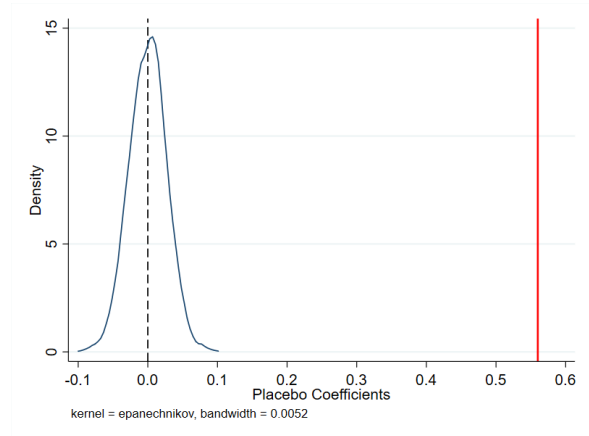
(b) Effects on O₃ Concentrations

Figure A1: Effects of Urban-Biased Monitoring on Pollutant Concentration at Different Distances from Urban Areas

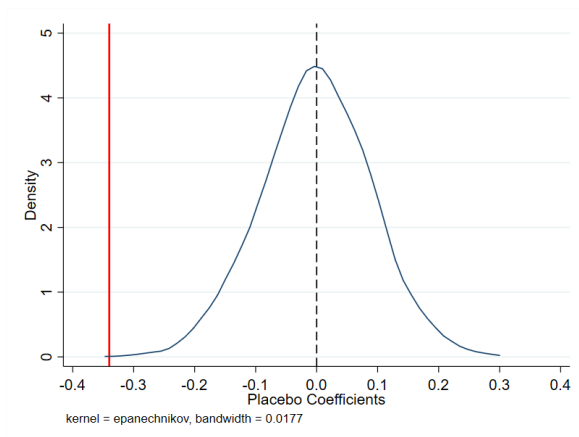
Notes: This figure plots the estimated coefficients and their 95% level confidence intervals for the effects of urban-biased monitoring policy on the PM_{2.5} and O₃ concentrations at different distance bins from the urban areas. Each point estimate represents the pollution change in each distance bin relative to the baseline group (the urban grids are taken as the baseline group here). The regressions include grid fixed effects, city-year fixed effects and meteorological control variables. Standard errors are clustered at the grid level.



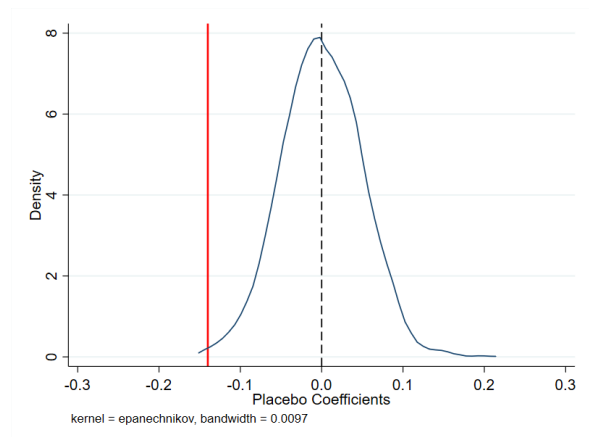
(a) Placebo Test for $PM_{2.5}$



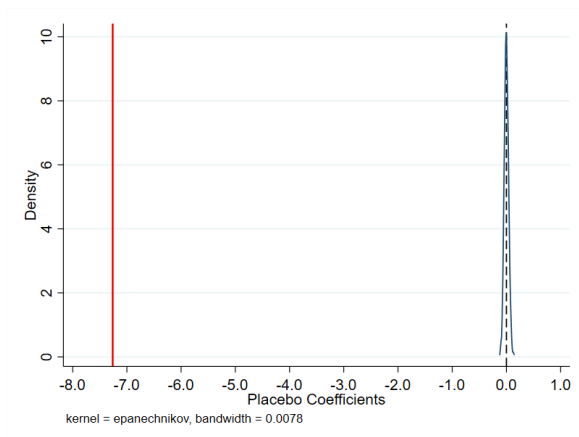
(b) Placebo Test for O_3



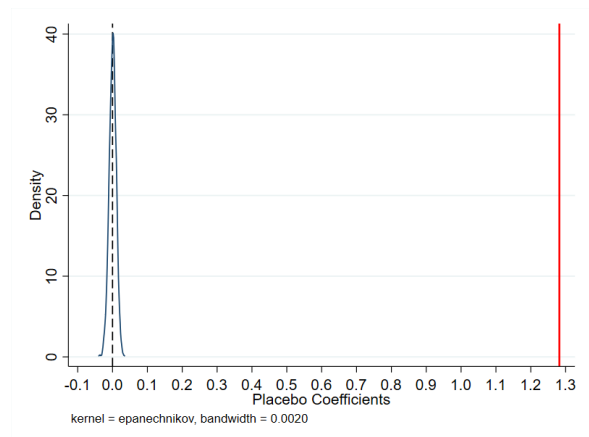
(c) Placebo Test for Bird Abundance



(d) Placebo Test for Bird Species Richness



(e) Placebo Test for $PM_{2.5}$ -Attributed Deaths



(f) Placebo Test for O_3 -Attributed Deaths

Figure A2: Placebo Tests

Notes: This figure presents the results of placebo tests. Figure (a), (b), (c), (d), (e), and (f) plot the placebo test for pollutant concentrations, bird diversity and pollutant-attributed deaths separately. We randomly assign treatment grids (areas) and randomly generate policy timing within the sample period for each city while keeping the mean value of variables *treat* and *post* unchanged. For each placebo test, the DID estimation is repeated 2000 times. The kernel density of the placebo estimates from the 2000 runs (blue lines) is then plotted along with the benchmark estimate (red line).

B Details on Variable Construction

We collect and construct a comprehensive dataset covering environmental and ecological domains, including the phased implementation timeline of pollution monitoring policies, urban area boundaries, PM_{2.5} and O₃ concentrations, anthropogenic emission inventories, and biodiversity data.

B.1 Core Explanatory Variables

B.1.1 National Air Quality Monitoring Policy Data

The precise geographic locations of all national monitoring stations were obtained from the National Urban Air Quality Real-Time Release Platform. Using announcement documents from the Ministry of Ecology and Environment (MEE), the specific year each prefecture-level city was first included in this network was compiled to construct the variable $post_{ct}$.

B.1.2 Urban–Rural Classification Data and Urban Area Variable Construction

The global urban built-up area dataset constructed by [Zhao et al. \(2021\)](#) is used to identify urban and rural areas. This dataset integrates multi-source remote sensing data such as nighttime light brightness and population density, applying a unified, objective standard to identify global urban built-up areas from 1992 to 2020. It demonstrates high reliability in characterizing the spatial distribution of high-density human activities and socio-economic intensity and maintains good consistency and comparability at the national scale.

Based on the 2012 urban built-up area data, the following spatial matching procedure was used to define urban and rural grids: using the Zonal Statistics tool in ArcGIS, the number of urban pixels within each $0.1^\circ \times 0.1^\circ$ grid cell was calculated. If the number of urban pixels within a grid was greater than zero, the grid was classified as an urban grid; otherwise, it was classified as a rural grid. Consequently, our definition of urban grids encompasses the built-up areas of prefecture-level city districts and the urban built-up areas of some county-level administrative units.

Furthermore, to ensure the robustness of the results and to delve deeper into the policy's ecological effects, we also constructed an alternative urban–rural classification scheme

based on administrative-spatial units. Specifically, we used the ArcGIS Raster-to-Polygon conversion tool to convert the urban built-up area raster data into vector polygons, and then merged all built-up area patches within the same city into a single urban polygon through a spatial dissolve operation; the remaining areas were defined as rural. Based on this classification scheme, we conducted supplementary analyses using a three-dimensional “city–area (urban/rural)–year” panel.

B.2 Outcome Variables

B.2.1 Air Pollutant Concentration Data

Pollutant concentration data come from the China High Air Pollutants (CHAP) dataset.²³ This dataset integrates ground monitoring, satellite remote sensing, atmospheric reanalysis, and numerical model simulation information, providing long-term, high-resolution surface air pollutant concentration products covering the whole of China, with high data quality and spatial consistency.

This study uses the annual average concentration data for PM_{2.5} and O₃ from the CHAP dataset for 2010–2019, with a spatial resolution of 1 km × 1 km. Using the ArcGIS Zonal Statistics function, the original data were aggregated to a 0.1° × 0.1° grid scale, calculating the average value within each grid cell. As a supplement, we also use data from the Multi-resolution Emission Inventory for China (MEIC) model developed by Tsinghua University. This dataset provides anthropogenic emission inventories for major air pollutants in China since 1990. We extract annual emission data for PM_{2.5}, SO₂, NO_x, and VOCs, with a spatial resolution of 0.25° × 0.25°.

B.2.2 Biodiversity Data

This paper uses bird observation data to construct proxy variables for biodiversity, quantifying ecosystem health. The data source is the China Bird Watching Records Center²⁴—a national citizen science project. As the largest open bird watching information system in China, this platform aggregates a massive number of observation records uploaded by reg-

²³See: <https://weijing-rs.github.io/product.html>.

²⁴See: <http://www.birdreport.cn/>

istered users. Its extensive geographical coverage (spanning over 2,200 counties) and species diversity (covering over 90% of bird species in China) provide a valuable data foundation for this study. Based on research needs, we extracted 44,051 bird watching records from 2010 to 2019, containing key information such as observation time, geographic coordinates, number of participants, bird count, and number of species.

However, the spatial discontinuity of bird observation data poses a methodological challenge. Conducting the analysis at a grid level would result in a substantial loss of valid samples due to missing records, introducing significant sample selection bias. To overcome this limitation, we conduct our analysis of bird diversity at the city-area-year level. We divide each prefecture-level city into a treatment urban area and a control rural area based on [Zhao et al. \(2021\)](#), and assign all bird observations accordingly based on their geographic coordinates. This approach offers a dual advantage: it mitigates data sparsity through spatial aggregation, while ensuring analytical consistency between our frameworks for biodiversity and pollutant concentration. By comparing the differences in changes in bird diversity between urban and rural areas, we can clearly identify the ecological consequences of the policy.

C China's National Air Quality Monitoring System

C.1 The Roll-out of the Monitoring System

China's national air quality monitoring system was established beginning in 2013, enabling comprehensive monitoring of six major air pollutants (PM_{2.5}, PM₁₀, O₃, CO, NO₂, and SO₂). The rollout proceeded in three phases.

Phase I (2013). 496 new or upgraded monitoring stations were established in 74 cities, implementing the new air quality standards and releasing pollutant concentrations in real time starting in 2013. These stations covered key regions such as the Beijing–Tianjin–Hebei region, the Yangtze River Delta, the Pearl River Delta, as well as municipalities directly under the central government and provincial capitals.

Phase II (2014). An additional 884 monitoring stations were added in 161 cities designated as key cities for environmental improvement or National Environmental Protection Model Cities, implementing the new air quality standards and releasing pollutant concentrations in real time starting in 2014.

Phase III (2015). The system was expanded to the remaining cities. By the end of 2014, a total of 1,436 national air quality monitoring stations had been established in 338 prefecture-level cities nationwide, with real-time implementation of the new air quality standards and pollutant reporting beginning in 2015. Their spatial distribution is shown in Figure C1.

The system serves two main functions.

Policy and performance evaluation: Monitoring data are used to assess whether prefecture-level cities meet pollution-reduction targets and air-quality improvement goals, and they play a key role in performance evaluations of government officials.

Data ownership and public transparency: The Ministry of Ecology and Environment (MEE), under the State Council, owns and maintains the stations; data are transmitted in real time to the China National Environmental Monitoring Centre and made public.

C.2 Spatial Layout of National Air Monitoring Stations.

The placement of air quality monitoring stations follows strict technical standards. According to the *Technical Regulation for Ambient Air Quality Monitoring Station Layout (Trial)*

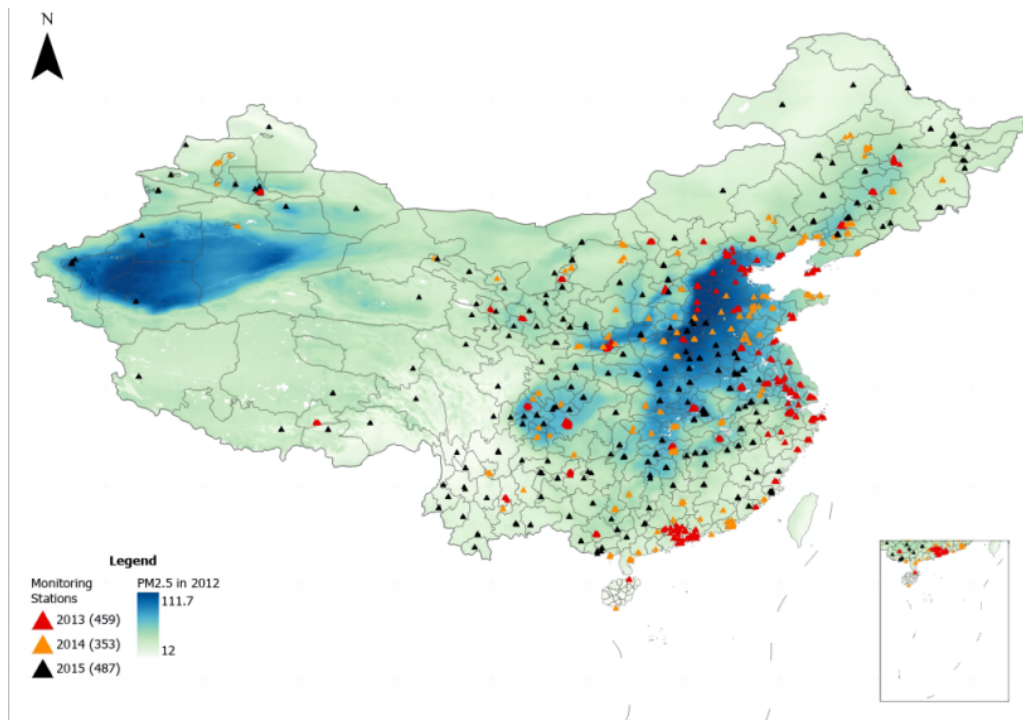


Figure C1: National Monitoring Sites and Spatial Distribution of PM_{2.5}

Note: The figure shows PM_{2.5} pollution in China in 2012 and the year in which each city's national monitoring stations began implementing the new air quality standards. PM_{2.5} units are micrograms per cubic meter.

(HJ 664–2013), monitoring stations must be evenly distributed based on the geographic scope of the urban built-up area and population.²⁵ In principle, station placement must meet three key criteria: representativeness (accurately reflecting air quality conditions and patterns), comparability (allowing for consistent data comparison), and comprehensiveness (considering environmental factors alongside socio-economic issues).

Figure C2 shows the geographic layout of monitoring stations relative to city boundaries and intra-city PM_{2.5} concentrations. It is noteworthy that the conceptual geographic spatial unit for Chinese prefecture-level cities can be defined in three ways: the entire administrative area, the urban district area, and the urban core or built-up area. As shown in Figure C2, for cities like Beijing and Chengdu that started monitoring in 2013, most stations are located within the urban core and are strategically placed in areas with higher pollution levels (panels a and b in Figure C2). Similarly, in Zibo and Luzhou (started monitoring in 2014) and Liaoyang and Huainan (started monitoring in 2015), monitoring stations are pri-

²⁵For example, cities with a population exceeding 3 million and a built-up area greater than 200 square kilometers require one monitoring station per 25–30 square kilometers, with a minimum of 8 stations. The coverage radius of each station ranges from 500 meters to 4 kilometers.

marily located within the urban core and strategically placed in areas with higher pollution (panels c–f in Figure C2). In summary, due to higher pollution levels and greater population density in urban areas, national air quality monitoring stations are typically located within urban cores, with very few or no stations in rural areas. Accompanying the monitoring system is the public release of real-time monitoring data online, providing citizens with timely information and enabling national authorities to assess urban pollution trends for environmental target evaluation.

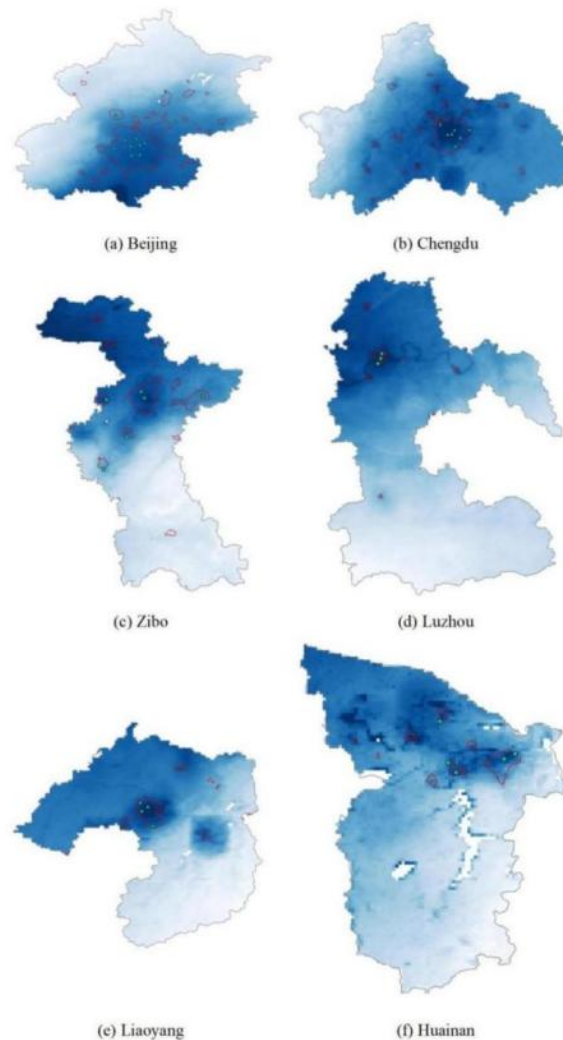


Figure C2: Urban Cores, Monitoring Site Locations, and PM_{2.5} Distribution in Prefecture-level Cities

Notes: This figure shows the urban core, monitoring site locations, and PM_{2.5} distribution for prefecture-level cities. Dots on the map represent monitoring stations, red lines delineate the urban core, and the background image represents PM_{2.5} concentration, where bluer colors indicate more severe pollution. Panels (a) and (b), (c) and (d), and (e) and (f) correspond to cities that began implementing the monitoring plan in 2013, 2014, and 2015, respectively.

D Separation of Two Scientific Pathways for O₃ Deterioration

We have illustrated in Section 2.2 that there are primarily two scientific pathways for the substitution between PM_{2.5} and O₃ based on the scientific literature. One is the uneven reduction of ozone precursor pollutants (NO_x and VOCs), the other is the physicochemical effect of PM_{2.5} reductions. Separating these two pathways is important because it can help us quantify what proportion of the increase in O₃ caused by the policy is due to improper management of precursor pollutants and what proportion is caused by the policy-induced PM_{2.5} declines. We conduct a simple and intuitive regression framework to separate these two pathways. The intuition of this frame is to separate the influence of NO_x and VOCs (the common precursor of O₃ and PM_{2.5}) on O₃ and the influence of PM_{2.5} itself on O₃. We combine the pollutant remote sensing data and the MEIC emission data to obtain the average concentrations of pollutants and the total emissions of precursor pollutants. The analysis is conducted at the 0.25° × 0.25° grid-year level (the same as Table 4).

$$PM_{it} = \alpha SO2_{it} + f(NOx_{it}, VOCs_{it}) + \boldsymbol{\theta}^\top X_{acy} + D_i + D_{ct} \quad (\text{D.1})$$

$$Ozone_{it} = \beta \widehat{PM}_{it} + f(NOx_{it}, VOCs_{it}) + \boldsymbol{\theta}^\top X_{acy} + D_i + D_{ct} \quad (\text{D.2})$$

The generation process of PM_{2.5} is modeled by Equation (D.1), where i represents the grid, t represents the year. PM_{it} is the grid-year level average PM_{2.5} concentrations. $SO2_{it}$, NOx_{it} and $VOCs_{it}$ represent the total emission of each precursor pollutant in grid i , year t . Other settings are the same as Equation (1). Based on the scientific literature, we characterize the relationship between SO₂ and PM_{2.5} as linear, and the relationship between NO_x, VOCs and PM_{2.5} as nonlinear. To operationalize the estimation, we incorporate the squared terms, interaction terms, and the linear terms of NOx_{it} and $VOCs_{it}$ into the regression. We predict the PM_{2.5} concentrations based on the estimation results of Equation (D.1) and eliminate the effects of NO_x and VOCs. Furthermore, we add the predicted PM_{2.5} concentrations (with the effects of NO_x and VOCs excluded) into Equation (D.2). The coefficient β reflects the

physicochemical relation between $\text{PM}_{2.5}$ and O_3 expressed by the second pathway.

The estimation results of Equation (D.1) and (D.2) are shown in Table A6. The results show that the physicochemical relationship between $\text{PM}_{2.5}$ and O_3 is approximately -0.721, indicating that when excluding the effects of NO_x and VOCs, a $1 \mu\text{g m}^{-3}$ decrease in $\text{PM}_{2.5}$ concentration is associated with approximately a $0.721 \mu\text{g m}^{-3}$ increase in O_3 concentration, on average. Combined with the baseline results in Table 1, we are able to conduct a back-of-the-envelope calculation of the overall effects of these two pathways on O_3 deterioration. The PM-targeted policy has led to a relative $0.573 \mu\text{g m}^{-3}$ decrease in $\text{PM}_{2.5}$ concentrations in urban areas compared to rural areas. The physicochemical relationship between $\text{PM}_{2.5}$ and O_3 will induce an average increase of approximately $0.412 \mu\text{g m}^{-3}$ in urban areas²⁶. This estimation indicates that the physicochemical relationship contributes approximately 73.8% of the policy-induced O_3 deterioration²⁷. The remaining 26.2% is contributed²⁷ by the uneven reduction of NO_x and VOCs. The separation results here are consistent with the scientific literature. For instance, the analysis by Li et al. (2019) suggests that for the rising O_3 trend in the North China Plain during the War on Pollution, the second scientific pathway was a more primary driver than changes in precursor emissions.

Our separation here has important policy implications. It indicates that when local governments focus only on $\text{PM}_{2.5}$, even if the levels of the precursor pollutants of O_3 remain unchanged, the O_3 pollution will still deteriorate due to the physicochemical relationship between $\text{PM}_{2.5}$ and O_3 . Moreover, increases in O_3 will cause significant deterioration of both human and ecological health, inducing unseen but long-term threatening social costs that partially offset the benefits of the $\text{PM}_{2.5}$ decline. The findings here suggest collaborative governance strategies for multiple pollutants. To comprehensively enhance air quality, the government must incorporate multiple pollutants into the assessment indicators simultaneously, thereby achieving coordinated control of multiple pollutants. Otherwise, the benefits of single-target governance may be partially offset by the pollutant substitution phenomenon triggered by the interaction between government incentives and scientific mechanisms, causing unseen but more threatening consequences.

²⁶ $-0.573 \mu\text{g m}^{-3} \times -0.721 = 0.413 \mu\text{g m}^{-3}$.

²⁷ $0.413 \mu\text{g m}^{-3} / 0.560 \mu\text{g m}^{-3} \approx 73.8\%$.

E Construction of Bird Diversity Indicators

E.1 Estimation Framework.

This paper uses citizen science data from the China Bird Report Center to construct proxy variables for biodiversity, quantifying ecosystem health. A key econometric challenge is that raw bird counts are influenced by observation effort (e.g., duration, number of observers) and observation conditions (e.g., weather, season). Using raw counts directly would introduce significant measurement error. To address this, we follow the approach of [Liang et al. \(2020\)](#), using observation–event–level data and regression analysis to isolate the effects of observation effort and conditions, thereby constructing a measure of bird abundance. Specifically, we estimate the following model:

$$birds_{icohdmy} = \exp\left(\beta_a hours_{icohdmy} + \beta_n observers_{icohdmy} + f_h + f_m + \Gamma_{icy} + \varepsilon_{icohdmy}\right), \quad (\text{E.1})$$

where i denotes the area type (urban/rural), c denotes the prefecture–level city, o denotes the bird watching team, h denotes the hour of the day,²⁸ d denotes the day of the month, m denotes the month of the year, and y denotes the year. $birds_{icohdmy}$ is the number of birds observed by team o in area i of city c at hour h on day d of month m in year y ; $hours_{icohdmy}$ is the total duration (in hours) of that observation event; and $observers_{icohdmy}$ is the total number of observers in the bird watching team. f_h is the hour–of–day fixed effect (capturing diurnal activity and observation behavior), f_m is the month fixed effect (capturing seasonal differences), and Γ_{icy} is the city–area–year fixed effect, measuring the relative level of bird abundance after controlling for the above factors and serving as our measure of interest for bird abundance. $\varepsilon_{icohdmy}$ is the error term. Since the dependent variable is a count variable, we estimate Equation (E.1) using Poisson Pseudo Maximum Likelihood (PPML). Analogously, we can obtain the bird species richness indicator by changing the dependent variable in equation (E.1) to the number of observed bird species.

There might be concerns that the citizen-science data source of bird observations is unevenly sampled. For example, the number of observations in some cities is significantly high

²⁸Determined by the *start time* of the observation. For example, if an observation starts at 9:40 AM, the event is assigned to the 9 AM hour.

or low, which will challenge the validity of our indicator. While it is worth noting that we address this issue by using the city-area-year fixed effects in equation (E.1) as the indicator, which captures the relative changes in bird abundance across cities, areas, and time. Importantly, because our goal is to estimate how bird abundance changes with environmental regulation and pollutant concentrations, rather than bird abundance *per se*, the construction of our indicator is both simple and valid.

E.2 Data Processing and Indicator Construction.

To implement the above estimation, we performed the following standardization procedures on the raw bird watching records:

Definition of Observation Event. Records from the same observation time and location are identified as belonging to the same observation event (i.e., the same observation team o). For each event, we calculate the total duration, total number of participants, total number of birds observed, and total number of species observed.

Urban–Rural Area Division. The administrative boundary of each prefecture–level city is divided into two macro–areas, “urban” and “rural”, based on Zhao et al. (2021) and all bird observation records are classified according to their geographic coordinates. Based on this, we construct biodiversity indicators using the “city–area–year” unit of analysis.

Data Cleaning. Considering potential recording errors from manual uploads in citizen science data and the influence of extreme observations, we winsorize the dependent variable (bird count) and key control variables (observation duration) at the top and bottom 1% before regression.

After data processing, we estimate Equation (E.1) using PPML and extract the estimated fixed effects $\hat{\Gamma}_{icy}$ as our primary biodiversity indicator—the *Bird Abundance Index*. Additionally, to measure species diversity, we replace the dependent variable in Equation (E.1) with the number of bird species observed and construct the *Bird Species Richness Index* through the same procedure. It is crucial to emphasize that the abundance indices estimated through this framework are *relative* measures. They reflect the deviation of a city–area–year from the

average level of all city–area–years in the sample period, after standardizing for observation conditions. Since the core objective of this study is to identify the impact of pollution control policies on the *relative* urban–rural gap in biodiversity (rather than its absolute level), this standardized relative measure is both appropriate and provides a more effective and reliable basis for causal inference after controlling for measurement error. Finally, we construct a three-dimensional panel dataset at the city–area (urban/rural)–year level for the empirical analysis in the main text.

Furthermore, the bird abundance and bird species richness indicators at the city–area–year–ecological guild level used in Section 5.3 of the main text are obtained based on the following equation:

$$\text{birds}_{icohdmy} = \exp\left(\beta_a \text{hours}_{icohdmy} + \beta_n \text{observers}_{icohdmy} + f_h + f_m + \Gamma_{ijcy} + \varepsilon_{icohdmy}\right), \quad (\text{E.2})$$

where j denotes the ecological guild, Γ_{ijcy} is the city–area–year–ecological guild fixed effect, and all other settings are consistent with Equation (E.1). We estimate Equation (E.2) using PPML and use the estimated coefficients for Γ_{ijcy} as measures of bird amount/species abundance for different ecological guilds at the city–area–year level.

F Impact of Monitoring Policy on Bird Diversity—Evidence at the City–Area–Year Level

F.1 Empirical Framework.

Due to the limitations of the bird watching data, the bird abundance indicator is difficult to estimate at the grid level. Therefore, all analyses involving bird abundance in the main text are conducted at the city-area-year level. That is, we construct the following empirical model:

$$bird_{icy} = \beta treat_i \times post_{cy} + \boldsymbol{\theta}^\top X_{icy} + f_{ic} + f_{cy} + \varepsilon_{icy}, \quad (\text{F.1})$$

where i represents the area (urban or rural), c represents the city, and y represents the year. $bird_{icy}$ is the bird abundance or bird species richness for area i in city c in year y , constructed as detailed in Appendix E; $post_{cy}$ is a dummy variable for the air pollution monitoring policy, taking the value 1 if city c had implemented the pollution monitoring policy in year y , and 0 otherwise; $treat_i$ is a dummy variable for treatment areas, taking the value 1 if area i is urban, and 0 otherwise; since meteorological conditions significantly affect bird life activities, we also include a set of city-year level meteorological control variables X_{icy} , including annual average maximum temperature, including annual average minimum temperature, and annual average precipitation; f_{ic} is the city-area (urban or rural) fixed effect, controlling for time-invariant unobservable characteristics at the city-area level, such as ecological environment features, topography, and climate type; f_{cy} is the city-year fixed effect, controlling for unobservable factors at the city-year level, such as climate fluctuations in special cities in particular years. Standard errors are clustered at the city-area level. β is the coefficient of interest, representing the change in bird abundance in urban areas relative to rural areas induced by the pollution monitoring policy.

F.2 Mechanism Analysis Framework for Unintended Ecological Damage.

Equation (F.1) can only depict the causal effect of the target-based environmental regulation policy on bird abundance but cannot reveal the underlying mechanism. To provide more solid empirical evidence for Hypothesis 4, we construct the following two-stage re-

gression framework to isolate the heterogeneous changes in O₃ between urban and rural areas induced by the environmental regulation policy and then examine their impact on bird abundance. The research framework is as follows:

Stage 1 (predict policy-induced ozone changes):

$$ozone_{icy} = \delta treat_i \times post_{cy} + \boldsymbol{\theta}^\top X_{icy} + f_{ic} + f_{cy} + \varepsilon_{icy}, \quad (\text{F.2})$$

Stage 2 (link pollutants to biodiversity):

$$bird_{icy} = \beta_{ozone} \widehat{ozone}_{icy} + \boldsymbol{\theta}^\top X_{icy} + f_{ic} + f_{cy} + \varepsilon_{icy}. \quad (\text{F.3})$$

In Equation (F.2), $ozone_{icy}$ is the average O₃ concentration at the city-area-year level, and other settings are the same as in Equation (F.1). In Equation (F.3), \widehat{ozone}_{icy} is the predicted average O₃ concentrations based on the regression results of Equation (F.2); other settings are the same as in Equation (F.1). Standard errors are clustered at the city-area level. β_{ozone} is the coefficient of interest, representing the impact of changes in ozone pollutions induced by the PM-targeted policy on bird diversity.

F.3 Impact of the Policy on Pollutant Concentrations—City–Area–Year Evidence.

To further ensure robustness, we also replicate the baseline results from the main text at the city-area-year level to demonstrate the robustness of the main conclusions and the rationale behind the research design involving bird abundance.

The results in Table A3 show that the estimated coefficients for the interaction term are significantly negative in Columns (1) to (3) and significantly positive in Columns (4) to (6), indicating that after policy, PM_{2.5} concentrations decreased significantly in urban areas relative to rural areas, while O₃ concentrations increased significantly. These results not only confirm the robustness of the grid-level regression results in the main text but also provide a solid empirical foundation for the design of the bird abundance analysis.

G Impact of the Monitoring Policy on General Biodiversity

G.1 Data and Sample Construction

The Biodiversity Intactness Index (BII) is a metric designed to assess the degree to which ecosystems are intact and functioning relative to their natural state. It measures the abundance and diversity of species in a given area compared to what would be expected in an undisturbed ecosystem. The BII accounts for various factors, including habitat loss, fragmentation, and degradation, providing a comprehensive view of biodiversity health. A higher BII value indicates a more intact ecosystem with greater species diversity and abundance, while a lower value suggests significant ecological disruption. This index was created by the Natural History Museum, London and uses their PREDICTS database, which currently contains over 3 million records from more than 26,000 sites across 94 countries, representing a diverse array of over 45,000 plant, invertebrate, and vertebrate species.

The BII includes geographic data with a resolution of $0.1^\circ \times 0.1^\circ$, for the years 2000, 2005, 2010, 2015, and 2020. We use the Zonal Statistics tool in ArcGIS to obtain the yearly mean value of BII for each grid.

G.2 Identification Strategy

To examine the impact of the monitoring policy on biodiversity, we estimate the following equation:

$$BII_{it} = \alpha \text{treat}_i \times \text{post}_{ct} + \gamma^T X_{act} + D_i + D_{ct} + u_{ict}, \quad (\text{G.1})$$

where i represents the grid, t represents the year, a represents the area (urban or rural), and c represents the prefecture-level city. BII_{it} is the mean value of biodiversity intactness index in grid i , year t . Other settings are the same as those in Equation (1). Because the BII data only includes the years 2000, 2005, 2010, 2015 and 2020, we estimate Equation (G.1) with the sample of these five years. Since the meteorological data from [Qin and Zhang \(2022\)](#) only cover up to 2019, we use the average meteorological values of other years as the observed meteorological values for 2020.

Further, we take the two-stage analytical framework introduced in Appendix F to inves-

investigate the impact of policy-induced O₃ on biodiversity:

Stage 1 (predict policy-induced ozone changes):

$$ozone_{it} = \delta treat_i \times post_{cy} + \boldsymbol{\theta}^\top X_{acy} + D_i + D_{ct} + \varepsilon_{it}, \quad (\text{G.2})$$

Stage 2 (link ozone changes to biodiversity):

$$BII_{it} = \beta_{ozone} \widehat{ozone}_{it} + \boldsymbol{\theta}^\top X_{acy} + D_i + D_{ct} + \varepsilon_{it}. \quad (\text{G.3})$$

In Equation (G.2), $ozone_{it}$ is the average O₃ concentrations at the grid-year level, and other settings are the same as in Equation (G.1). In Equation (G.3), \widehat{ozone}_{it} is the predicted average O₃ concentrations based on the regression results of Equation (G.2); other settings are the same as in Equation (G.1). Standard errors are clustered at the grid level. β_{ozone} is the coefficient of interest, representing the impact of changes in ozone concentrations induced by the PM-targeted policy on biodiversity. The results are reported in Table A7.

H Conceptual Framework

This appendix develops an equilibrium model of targeted pollution regulation that formalizes the pollutant substitution mechanism and derives testable predictions. The model features two strategic agents — firms choosing abatement levels and a local government allocating enforcement effort across pollutant sources — and two ambient pollutants: $\text{PM}_{2.5}$, which is targeted by policy, and O_3 , which is not.

H.1 Pollution Function

The firm emits three categories of precursors indexed by $j \in \{S, N, V\}$: sulfur dioxide (S , i.e., SO_2), nitrogen oxides (N , i.e., NO_x), and volatile organic compounds (V , i.e., VOCs). SO_2 originates primarily from large point sources such as power plants and heavy industry. NO_x is produced by combustion processes across both large and dispersed sources. VOCs emanate from diffuse sources including solvent use, small industrial operations, and transportation.

Ambient $\text{PM}_{2.5}$ is increasing in all precursor emissions:

$$P(\mathbf{e}) = \sum_{j \in \{S, N, V\}} \alpha_j e_j, \quad \alpha_j > 0 \quad \forall j, \quad (\text{H.1})$$

where e_j denotes the emission level of precursor j and α_j is the marginal contribution of precursor j to ambient $\text{PM}_{2.5}$. SO_2 and NO_x are major precursors of secondary inorganic aerosols (sulfate and nitrate), which typically account for a large fraction of $\text{PM}_{2.5}$ mass. In contrast, while VOCs contribute to secondary organic aerosol formation, the effective mass yield from VOCs oxidation is generally lower and more uncertain. We therefore assume that the marginal contribution of SO_2 and NO_x to ambient $\text{PM}_{2.5}$ exceeds that of VOCs: $\alpha_S, \alpha_N > \alpha_V$.

Ambient O_3 depends on the emissions of its photochemical precursors (NO_x and VOCs) and on the ambient $\text{PM}_{2.5}$ concentration. This formulation reflects two distinct scientific

pathways discussed in Section 2:

$$O(\mathbf{e}) = \underbrace{g(e_N, e_V)}_{\text{behavioral pathway}} - \underbrace{\gamma \cdot P(\mathbf{e})}_{\text{physicochemical pathway}}, \quad (\text{H.2})$$

where $\gamma > 0$ since higher $\text{PM}_{2.5}$ concentrations suppress O_3 . Atmospheric particulates provide surfaces that scavenge hydroperoxyl radicals (HO_2), which are crucial for O_3 formation. As $\text{PM}_{2.5}$ declines, these radicals persist in the atmosphere and accelerate O_3 production.

The function $g(e_N, e_V)$ captures the behavioral pathway. In the VOC-limited chemical regime characteristic of Chinese urban atmospheres, higher VOC emissions accelerate O_3 formation, while higher NO_x emissions suppress O_3 through the titration effect ($\text{NO} + \text{O}_3 \rightarrow \text{NO}_2 + \text{O}_2$), which dominates over NO_x 's role as an O_3 precursor in the high- NO_x urban regime. Therefore, we assume that $\partial g / \partial e_V > 0$ and $\partial g / \partial e_N < 0$. For tractability, we adopt a linear specification $g(e_N, e_V) = \beta_V e_V - \beta_N e_N$ with $\beta_V, \beta_N > 0$. Substituting into (H.2) implies that:

$$O(\mathbf{e}) = (\beta_V - \gamma \alpha_V) e_V - (\beta_N + \gamma \alpha_N) e_N - \gamma \alpha_S e_S, \quad (\text{H.3})$$

where we assume $\beta_V > \gamma \alpha_V$, ensuring that the direct effect of VOCs on O_3 is positive.

H.2 Firms and Local Governments

Firms: The firm operates with pre-policy baseline emissions $\bar{\mathbf{e}} = (\bar{e}_S, \bar{e}_N, \bar{e}_V)$ and chooses abatement levels $\mathbf{a} = (a_S, a_N, a_V) \geq 0$, so that realized emissions are $e_j = \bar{e}_j - a_j$. Given an emission tax τ_j on precursor j , the firm minimizes total abatement costs net of the implicit emissions tax:

$$\min_{\mathbf{a} \geq 0} \sum_j \frac{1}{2} \kappa_j a_j^2 - \sum_j \tau_j a_j, \quad (\text{H.4})$$

where $\kappa_j > 0$ is the marginal cost parameter for abating precursor j . The firm's optimal abatement under the emission tax τ is:

$$a_j^*(\tau_j) = \frac{\tau_j}{\kappa_j}. \quad (\text{H.5})$$

Stronger enforcement (i.e., a higher τ_j) induces greater abatement. Substituting $e_j = \bar{e}_j - a_j^*$ into the pollution functions yields ambient concentrations as functions of the regulatory enforcement intensities (i.e., emission tax τ) set by the local government:

Local Governments: The local government chooses enforcement intensities $\tau = (\tau_S, \tau_N, \tau_V)$ across precursor sources. Enforcement is costly, and the cost reflects the administrative burden of monitoring heterogeneous sources:

$$C_L(\tau) = \sum_j \frac{1}{2} \eta_j \tau_j^2, \quad (\text{H.6})$$

where $\eta_j > 0$ is the marginal cost parameter for monitoring precursor j . The regulator operates under a finite enforcement budget $\sum_j \frac{1}{2} \eta_j \tau_j^2 \leq \bar{C}$, where $\bar{C} > 0$ reflects the total regulatory capacity (inspectors, monitoring equipment, administrative resources). This constraint is central to the model: it implies that intensifying enforcement on one precursor crowds out enforcement on others.

Subject to this budget constraint, the local government minimizes a weighted sum of ambient pollutants, placing weight λ on PM_{2.5} and weight ω on O₃:

$$\min_{\tau} \underbrace{\lambda \cdot P(\tau)}_{\text{loss from PM}_{2.5} \text{ damage}} + \underbrace{\omega \cdot O(\tau)}_{\text{loss from O}_3 \text{ damage}} \quad \text{s.t.} \quad \sum_j \frac{1}{2} \eta_j \tau_j^2 \leq \bar{C}, \quad (\text{H.7})$$

The associated Lagrangian is

$$\mathcal{L} = \lambda \cdot P(\tau) + \omega \cdot O(\tau) - \mu \left(\bar{C} - \sum_j \frac{1}{2} \eta_j \tau_j^2 \right), \quad (\text{H.8})$$

where $\mu \geq 0$ is the Lagrangian multiplier. Solving the first-order conditions yields the optimal enforcement intensities:

$$\tau_S^* = \frac{1}{\mu} \underbrace{(\lambda - \omega \gamma) \frac{\alpha_S}{\kappa_S \eta_S}}_{\equiv A_S}, \quad (\text{H.9})$$

$$\tau_N^* = \frac{1}{\mu} \underbrace{\left[(\lambda - \omega\gamma) \frac{\alpha_N}{\kappa_N \eta_N} - \omega \frac{\beta_N}{\kappa_N \eta_N} \right]}_{\equiv A_N}, \quad (\text{H.10})$$

$$\tau_V^* = \frac{1}{\mu} \underbrace{\left[(\lambda - \omega\gamma) \frac{\alpha_V}{\kappa_V \eta_V} + \omega \frac{\beta_V}{\kappa_V \eta_V} \right]}_{\equiv A_V}, \quad (\text{H.11})$$

where A_j represents the marginal benefit of increasing regulatory effort on precursor j , capturing the gains from reductions in both $\text{PM}_{2.5}$ and O_3 . For SO_2 , enforcement reduces $\text{PM}_{2.5}$ but indirectly increases O_3 through the physicochemical pathway, so the O_3 weight diminishes the enforcement benefit. For NO_x , enforcement additionally increases O_3 , further reducing the marginal benefit. Crucially, for VOCs, enforcement reduces O_3 directly, which adds to the marginal benefit. Substituting the above three equations into the budget constraint implies:

$$\mu = (2\bar{C})^{-\frac{1}{2}} \left(\sum_k \eta_k A_k^2 \right)^{\frac{1}{2}}. \quad (\text{H.12})$$

H.3 Predictions

We now examine the impact of an increase in λ (i.e., the regulator places greater emphasis on $\text{PM}_{2.5}$). Differentiating $\ln \tau_j^* = \ln A_j - \ln \mu$ with respect to λ implies:

$$\frac{d \ln \tau_j^*}{d\lambda} = \frac{1}{A_j} \frac{dA_j}{d\lambda} - \frac{\sum_k A_k \frac{\alpha_k}{\kappa_k}}{\sum_k \eta_k A_k^2}, \quad (\text{H.13})$$

where $\frac{dA_j}{d\lambda} = \frac{\alpha_j}{\kappa_j \eta_j}$ for all j . The first term captures the direct effect of increased $\text{PM}_{2.5}$ pressure, while the second term captures the indirect effect operating through the tighter budget constraint. After algebraic simplification, we have:

$$\frac{d \ln \tau_S^*}{d\lambda} = \frac{\omega}{A_S (\sum_k \eta_k A_k^2)} \left(A_V \frac{\alpha_S}{\kappa_S \eta_S} \frac{\beta_V}{\kappa_V} - A_N \frac{\alpha_S}{\kappa_S \eta_S} \frac{\beta_N}{\kappa_N} \right) \quad (\text{H.14})$$

$$\frac{d \ln \tau_N^*}{d\lambda} = \frac{\omega}{A_N (\sum_k \eta_k A_k^2)} \left(A_S \frac{\alpha_S}{\kappa_S} \frac{\beta_N}{\kappa_N \eta_N} + A_V \frac{\alpha_V}{\kappa_V} \frac{\beta_N}{\kappa_N \eta_N} + A_V \frac{\alpha_N}{\kappa_N \eta_N} \frac{\beta_V}{\kappa_V} \right) \quad (\text{H.15})$$

$$\frac{d \ln \tau_V^*}{d\lambda} = -\frac{\omega}{A_V (\sum_k \eta_k A_k^2)} \left(A_S \frac{\alpha_S}{\kappa_S} \frac{\beta_V}{\kappa_V \eta_V} + A_N \frac{\alpha_N}{\kappa_N} \frac{\beta_V}{\kappa_V \eta_V} + A_N \frac{\alpha_V}{\kappa_V \eta_V} \frac{\beta_N}{\kappa_N} \right) \quad (\text{H.16})$$

To guarantee the pollution emission of SO₂ decline when government more care about PM_{2.5}, we assume that $\frac{\beta_V}{\kappa_V} A_V - \frac{\beta_N}{\kappa_N} A_N > 0$, which implies:

Lemma 1. *As the regulator places greater emphasis on PM_{2.5} (higher λ), enforcement on SO₂ and NO_x increases, while enforcement on VOCs decreases:*

$$\frac{d \ln \tau_S^*}{d\lambda} > 0, \quad \frac{d \ln \tau_N^*}{d\lambda} > 0, \quad \frac{d \ln \tau_V^*}{d\lambda} < 0. \quad (\text{H.17})$$

Given the negative relationship between firms' equilibrium emissions and regulatory intensity ($e_j^* = \bar{e}_j - \tau_j^* / \kappa_j$), Lemma 1 directly implies:

Proposition 1. *When the regulator places a higher weight on PM_{2.5}, the accompanying adjustments in enforcement cause SO₂ and NO_x emissions to decrease, while VOC emissions rise:*

$$\frac{de_S^*}{d\lambda} < 0, \quad \frac{de_N^*}{d\lambda} < 0, \quad \frac{de_V^*}{d\lambda} > 0. \quad (\text{H.18})$$

Combining Proposition 1 with the pollution functions (H.1) and (H.3), we have the second proposition:

Proposition 2. *As the regulator becomes more concerned about the harm of PM_{2.5}, the asymmetric adjustment in precursor emissions leads to a decrease in PM_{2.5} concentrations and a simultaneous increase in O₃ concentrations:*

$$\frac{dP}{d\lambda} = \sum_j \alpha_j \frac{de_j^*}{d\lambda} < 0, \quad (\text{H.19})$$

$$\frac{dO}{d\lambda} = -\gamma\alpha_S \frac{de_S^*}{d\lambda} - (\beta_N + \gamma\alpha_N) \frac{de_N^*}{d\lambda} + (\beta_V - \gamma\alpha_V) \frac{de_V^*}{d\lambda} > 0. \quad (\text{H.20})$$

Proof. Given the ordering $\alpha_S, \alpha_N > \alpha_V$, the decrease in PM_{2.5} resulting from reductions in SO₂ and NO_x emissions dominates the opposing effect from increased VOCs. Thus, under the condition of a small α_V , heightened concern about PM_{2.5} results in a net decline in PM_{2.5}. In the case of O₃, all terms contributing to $dO/d\lambda$ are positive. It follows that $dO/d\lambda > 0$, indicating that greater concern for PM_{2.5} ultimately increases O₃ concentrations. \square